

Suppression of PKR Promotes Network Excitability and Enhanced Cognition by Interferon- γ -Mediated Disinhibition

Ping Jun Zhu,^{1,2} Wei Huang,^{1,2} Djanenkhodja Kalikulov,^{1,7} Jong W. Yoo,³ Andon N. Placzek,^{1,6} Loredana Stoica,^{1,2} Hongyi Zhou,^{1,2} John C. Bell,⁴ Michael J. Friedlander,^{1,7} Krešimir Krnjević,⁵ Jeffrey L. Noebels,³ and Mauro Costa-Mattioli^{1,2,*}

¹Department of Neuroscience

²Molecular and Cellular Biology, Center for Addiction, Learning, and Memory

³Department of Neurology

Baylor College of Medicine, Houston, TX 77030, USA

⁴Ottawa Health Research Institute, Ottawa K1H 8L6, Canada

⁵Physiology Department, McGill University, Montreal H3G 1Y6, Canada

⁶Present address: Division of Basic Medical Sciences, Mercer University School of Medicine, 1550 College Street, Macon, GA 31207, USA

⁷Present address: Virginia Tech Carilion Research Institute, Virginia Tech, Roanoke, VA 24016, USA

*Correspondence: costamat@bcm.edu

DOI 10.1016/j.cell.2011.11.029

SUMMARY

The double-stranded RNA-activated protein kinase (PKR) was originally identified as a sensor of virus infection, but its function in the brain remains unknown. Here, we report that the lack of PKR enhances learning and memory in several behavioral tasks while increasing network excitability. In addition, loss of PKR increases the late phase of long-lasting synaptic potentiation (L-LTP) in hippocampal slices. These effects are caused by an interferon- γ (IFN- γ)-mediated selective reduction in GABAergic synaptic action. Together, our results reveal that PKR finely tunes the network activity that must be maintained while storing a given episode during learning. Because PKR activity is altered in several neurological disorders, this kinase presents a promising new target for the treatment of cognitive dysfunction. As a first step in this direction, we show that a selective PKR inhibitor replicates the *Pkr*^{-/-} phenotype in WT mice, enhancing long-term memory storage and L-LTP.

INTRODUCTION

The double-stranded (ds) RNA-activated protein kinase (PKR) is widely present in vertebrates, and its activation leads to the phosphorylation of several substrates, the major known cytoplasmic target being the translation initiation factor eIF2 α (Dever et al., 2007). Although PKR is activated in response to a variety of cellular stresses, such as viral infection (García et al., 2007) and status epilepticus (Camevalli et al., 2006), and in several neuropathologies, including Alzheimer's (Couturier et al., 2010; Peel

and Bredesen, 2003), Parkinson's (Bando et al., 2005), Huntington's (Bando et al., 2005; Peel et al., 2001), and Creutzfeldt-Jakob's diseases (Paquet et al., 2009), little is known about its role in normal brain function.

Cognitive functions are believed to arise from the finely coordinated interactions of a large number of neurons widely distributed throughout the brain. A fundamental yet unresolved question of modern neuroscience is how optimal synchronization is achieved without degrading information flow. Though transient synchronizations of neuronal discharges have been proposed to promote memory consolidation (Beenhakker and Huguenard, 2009; Buzsaki, 2006; Girardeau et al., 2009; Paulsen and Moser, 1998), seizure activity can develop in hyperexcitable oscillatory networks (Huguenard and McCormick, 2007; Steriade, 2005). GABAergic synaptic transmission plays a pivotal role in maintaining this balance. GABAergic inhibitory neurons not only suppress the activity of principal cells, but also serve as a generator of oscillations in hippocampal networks (Freund, 2003; Klausberger and Somogyi, 2008; Mann and Mody, 2010; Sohal et al., 2009), which appear to be crucial for memory consolidation (Beenhakker and Huguenard, 2009; Buzsaki, 2006; Girardeau et al., 2009; Paulsen and Moser, 1998). Furthermore, GABAergic inhibition also helps to terminate these rhythmic events, thus preventing runaway epileptiform network activity. However, little is known about the molecular mechanisms critical for dynamically scaling GABAergic control of neuronal synchrony during memory formation.

A reduction of GABAergic synaptic transmission is classically associated with epileptiform activity (Beenhakker and Huguenard, 2009; Cossart et al., 2005; Noebels, 2003). Though many kinds of epilepsy lead to cognitive impairment (Holmes and Lenck-Santini, 2006), some seizure disorders spare memory, and a few rare forms have been associated with extraordinary mental abilities (Heaton and Wallace, 2004; Hughes, 2010). However, little is known about the causes or possible genetic

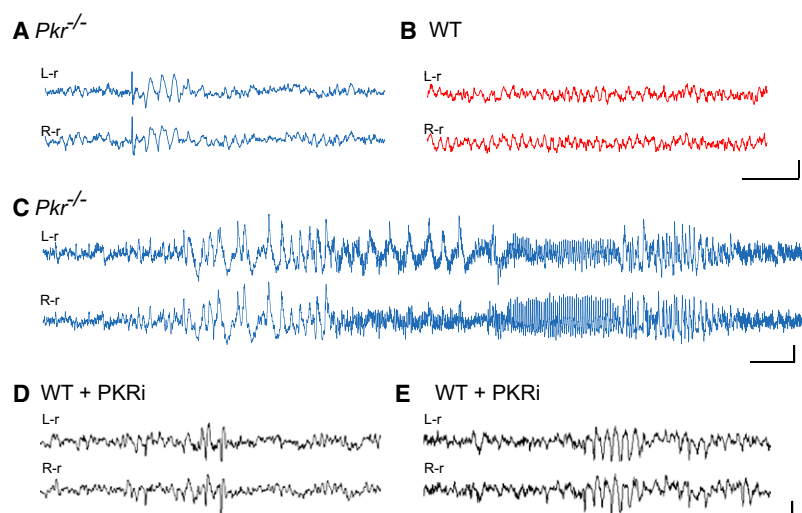


Figure 1. Synchronized EEG Activity in *Pkr*^{-/-} Mice or WT Mice Treated with PKRi In Vivo

(A–C) Traces from bilateral cortical electrodes (left hemisphere reference, L-r; right hemisphere reference, R-r) show abnormal synchronous activity, including solitary interictal spikes followed by brief wave discharges (A) and electrographic seizures (C) in freely moving *Pkr*^{-/-} mice, but not in WT mice (B).

(D and E) Injection of PKR inhibitor (PKRi; 0.1 mg/kg i.p.) induced acute spiking (D) and rhythmic bursts (E) in adult WT mice. Calibration: 1 s and 200 μ V. Abnormal EEG activity was absent from all WT control recordings ($n = 7$) but present in all *Pkr*^{-/-} mice ($n = 10$) and in six out of seven PKRi-injected mice (recorded 1 hr after of PKRi injection). By Fisher's exact test, p values were < 0.001 and < 0.01 , respectively.

For additional information, see [Movie S1](#). See [Figure S1](#) for lack of change in brain morphology; [Figure S6B](#) for EEG interictal spikes in mice with constitutively reduced eIF2 α phosphorylation (eIF2 α ^{+SS1A} mice); and [Figure S7D](#) for the effect of PKRi in vivo.

mutations associated with this type of epilepsy. Here, we report that loss of PKR or pharmacological inhibition of PKR activity promotes network hyperexcitability and enhances L-LTP and long-term memory (LTM). Importantly, we show that PKR regulates these processes via a selective control of GABAergic synaptic transmission mediated by interferon- γ (IFN- γ), uncovering a new molecular signaling pathway that regulates network rhythmicity, synaptic plasticity, and memory storage in the adult brain.

RESULTS

Deficient PKR Kinase Activity Leads to Synchronous Network Discharges In Vivo and In Vitro

PKR knockout (*Pkr*^{-/-}) mice are viable, fertile, and of normal size and are phenotypically indistinguishable from their wild-type (WT) littermates (Abraham et al., 1999). Nissl staining and synaptic markers for the vesicular glutamate transporter 1 (VGLUT1, a marker of presynaptic glutamatergic terminals), postsynaptic density protein 95 (PSD95, a marker of postsynaptic terminals), and glutamic acid decarboxylase 67 (GAD67, a marker of GABAergic terminals) show no gross abnormalities in *Pkr*^{-/-} mouse brain (Figures S1A–S1D available online). As expected, PKR protein is undetectable in *Pkr*^{-/-} brain, as determined by immunohistochemistry and western blotting (Figures S1E and S1F).

To determine whether PKR regulates network rhythmicity, we first monitored spontaneous cortical brain rhythms in freely moving WT and *Pkr*^{-/-} mice by simultaneous video and electroencephalogram (videoEEG) recording. In recordings from *Pkr*^{-/-} mice, we found intermittent abnormal spike discharges (Figure 1A; at a mean frequency of 40 ± 9 interictal spike/hr), as well as infrequent generalized electrographic seizures (Figure 1C; at a mean frequency of 1.1 ± 0.021 seizures/hr), that were not accompanied by convulsive behavioral manifestations. Neither abnormality ever appeared in the EEG from WT mice (Figure 1B). Simultaneous recordings from the neocortex and hippocampus from *Pkr*^{-/-} mice showed comparable epileptiform activity (see

Movie S1). Thus, loss of PKR leads to aberrant hyperactivity of neuronal networks. Because the excitability imbalance in *Pkr*^{-/-} mice might arise during development, we suppressed PKR activity acutely in adult WT mice by systemic administration of a selective PKR inhibitor (PKRi) (Jammi et al., 2003). Remarkably, the injections of PKRi rapidly induced both interictal spikes (Figure 1D; at a mean frequency of 25 ± 7.8 interictal spike/hr) and abnormal EEG rhythmic bursting activity (Figure 1E), like those occurring spontaneously in *Pkr*^{-/-} mice (compare Figure 1E to Figure 1A). As in the case of *Pkr*^{-/-} mice, the spontaneous discharges in PKRi-treated mice were not accompanied by changes in ongoing behavior. Together, these observations reveal a pivotal role for this kinase as a regulator of network rhythmicity.

To determine whether the abnormal synchronous network activity in *Pkr*^{-/-} mice or WT mice treated with PKRi could be recapitulated in vitro, we recorded field EPSPs (fEPSPs) and population spikes (in CA1) in hippocampal slices from WT and *Pkr*^{-/-} mice or in WT slices treated with PKRi. The population spike is a useful index of the responsiveness of many pyramidal neurons to excitatory inputs: its size reflects the neuron's intrinsic excitability as well as the balance between excitatory and inhibitory synaptic inputs. An appropriate single electrical stimulus applied to the stratum radiatum elicited a similar field EPSP and population spike in WT and *Pkr*^{-/-} slices (Figures 2A and 2B, insets). However, in the presence of a very low priming concentration of bicuculline (2 μ M), the same stimulus evoked a prominent after-discharge in *Pkr*^{-/-} slices, but not in WT slices (compare Figure 2A to 2B; see also Figures 2D and 2E), revealing a latent hyperexcitability of hippocampal networks in *Pkr*^{-/-} slices. A similar after-discharge was observed when PKRi was applied to WT slices (Figure 2C; see also Figures 2D and 2E), demonstrating a comparable increase in excitability when PKR was inhibited pharmacologically.

An increased tendency to fire spikes in *Pkr*^{-/-} slices was also revealed when field responses were elicited in CA1 by stimulating the afferent input over a wide range of intensities. Plots of afferent fiber volley (AV) versus stimulus intensity, initial slope

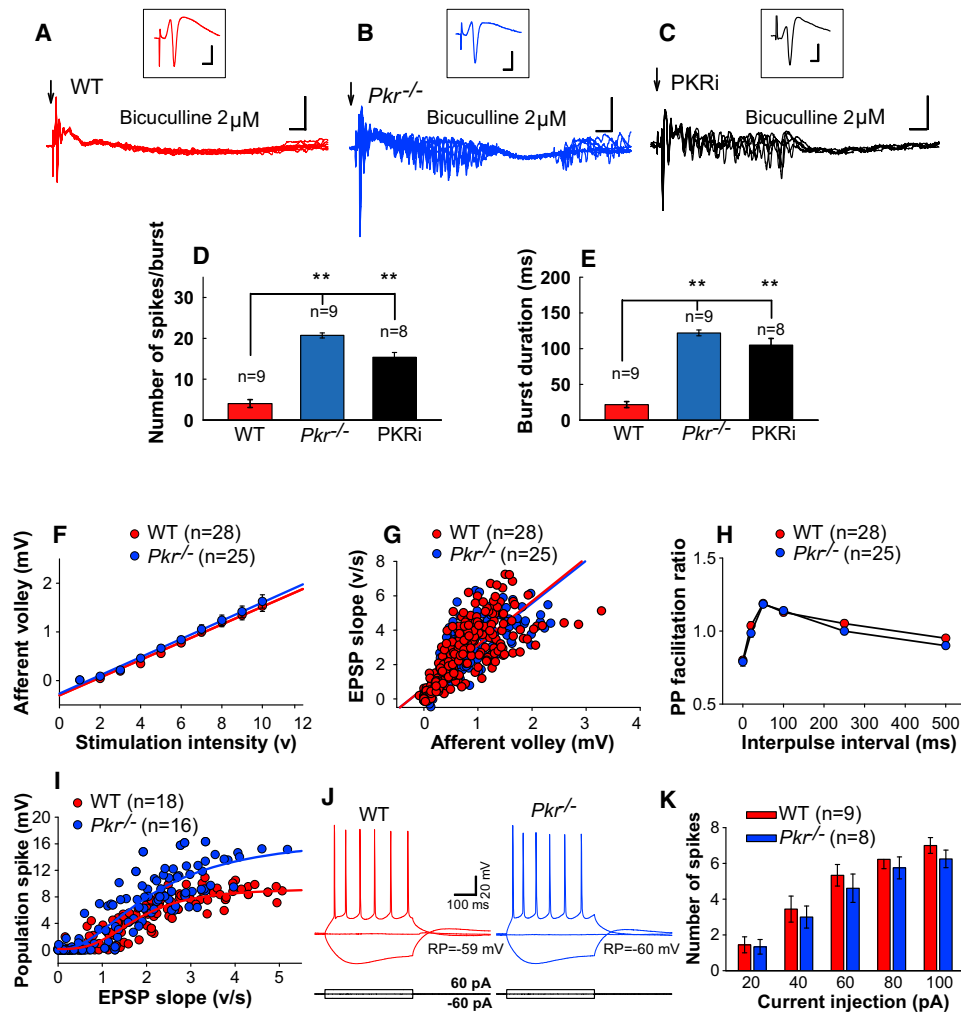


Figure 2. Synchronized Activity and Reduced Inhibition in *Pkr*^{-/-} Hippocampal Slices or WT Slices Treated with PKRi

(A–C) Population spikes were elicited by half-maximal electrical stimulation at 0.03 Hz (indicated by arrow). Insets in (A), (B), and (C) are averaged traces recorded before applying a very low concentration of bicuculline (2 μ M), which generated pronounced after-discharges in *Pkr*^{-/-} slices (B) or WT slices treated with PKRi (1 μ M) (C), but not in WT slices (A). For all plots, $n \geq 5$; calibrations: 2 ms and 3 mV for insets and 10 ms and 5 mV for slow traces.

(D and E) Compared to WT slices, the number of evoked spikes (D, $F_{(2,24)} = 66.3$; ** $p < 0.01$) and the duration of burst (E, $F_{(2,24)} = 100.2$; ** $p < 0.01$) were increased in *Pkr*^{-/-} slices or WT slices treated with PKRi.

(F–K) Similar intrinsic neuronal properties and basal synaptic transmission but maximal fEPSPs elicited larger population spikes in *Pkr*^{-/-} slices.

(F) Input-output data show similar amplitudes of presynaptic fiber volleys over a wide range of stimulus intensities in WT and *Pkr*^{-/-} slices. Mean afferent volley versus stimulus strength were fitted by linear regression ($R^2 = 0.989$ for WT and 0.993 for *Pkr*^{-/-} slices).

(G) fEPSPs as a function of presynaptic fiber volley did not differ between WT and *Pkr*^{-/-} slices (linear regression; $R^2 = 0.643$ for WT and 0.638 for *Pkr*^{-/-} slices).

(H) Paired-pulse facilitation of fEPSPs did not differ between WT and *Pkr*^{-/-} slices, as shown by the plots of the PP ratio (fEPSP2/fEPSP1) for various intervals of paired stimulation.

(I) Sigmoidal relationship of population spikes versus fEPSP, though initially similar, reached a higher ceiling in *Pkr*^{-/-} slices.

(J and K) In whole-cell recordings in the presence of glutamate and GABA antagonists, resting membrane potential was -59 ± 1.23 mV for WT and -60 ± 1.22 mV for *Pkr*^{-/-} slices ($p > 0.05$), and input resistance was 397 ± 24 M Ω for WT and 381 ± 39 M Ω for *Pkr*^{-/-} slices ($p > 0.05$). Inward and outward current pulses generated similar voltages changes (J) and numbers of spikes (K) in WT and *Pkr*^{-/-} slices.

For information about the effect of PKRi in vitro, see Figure S7C.

of field EPSPs versus AV size, and paired-pulse facilitation (PPF) did not significantly differ between *Pkr*^{-/-} and WT slices (Figures 2F–2H), indicating no change in the excitability of afferent fibers or the efficacy of excitatory synaptic transmission in *Pkr*^{-/-} slices. Relatively small fEPSPs (<half-maximal) evoked similar population spikes in *Pkr*^{-/-} and WT slices (Figure 2I), indicating

no difference in intrinsic excitability of the postsynaptic cells. Hence, the intrinsic membrane properties and responsiveness of CA1 pyramidal neurons did not differ between WT and *Pkr*^{-/-} slices (Figures 2J–2K). However, fEPSPs elicited by stronger stimulation evoked larger population spikes in *Pkr*^{-/-} slices, thus reaching a higher ceiling in the sigmoidal relationship

between population spikes and fEPSPs (Figure 2I). Given that excitatory transmission was unchanged (Figure 2G), these data suggest that population spikes reached a higher ceiling in *Pkr*^{-/-} slices because inhibition was impaired. A comparable increase in the population spike amplitude ceiling is generated by a GABA antagonist (Chavez-Noriega et al., 1989). Accordingly, pharmacological inhibition of PKR (with PKRi) also enhanced population spikes (see Figures S3F and S3G).

Deficient PKR Kinase Activity Reduces Inhibitory Synaptic Transmission

Because impaired inhibition is a common feature of genetic models of epilepsy (Noebels, 2003), we asked whether this might account for the hyperexcitability observed in *Pkr*^{-/-} mice. To test this hypothesis, we studied inhibitory synaptic transmission in a series of experiments on hippocampal slices from WT and *Pkr*^{-/-} mice and WT slices treated with PKRi. In whole-cell patch-clamp recordings from CA1 neurons, the frequency (but not the amplitude) of both spontaneous and miniature inhibitory postsynaptic currents (sIPSCs and mIPSCs) was significantly reduced in *Pkr*^{-/-} slices (Figures S2A and 3A) or in WT slices treated with PKRi (Figures S2B and 3B). The absence of change in mIPSC amplitude or duration is a strong indication that PKR does not affect the sensitivity of pyramidal cells to synaptically released GABA. Next, we found that, in CA1 neurons from PKR-deficient slices (*Pkr*^{-/-} slices and PKRi-treated WT slices), the amplitude of evoked IPSCs was reduced over a wide range of stimulation intensities (Figures S2D and 3C). In contrast to its effect in WT slices, PKRi did not alter the amplitude of evoked IPSCs in *Pkr*^{-/-} slices (compare Figure 3D to 3E), confirming that its effect was not due to an off-target action. Providing evidence of reduced GABA release, paired-pulse depression, a sensitive index of changes in evoked GABA release (Thomson, 2000), was significantly decreased in PKR-deficient slices (Figure 3F). Moreover, PKR seems to regulate inhibitory transmission presynaptically, as there was no difference in the time course of mIPSCs and sIPSCs between WT slices and PKR-deficient slices (Figures 3A, 3B, S2A, S2B, and Table S1), which is consistent with a lack of change in postsynaptic receptor-related mechanisms.

Further evidence of less efficient cumulative GABAergic inhibition in PKR-deficient slices is the much better preservation of CA1 population spikes during high-frequency stimulation (compare Figure S3A to S3C and S3D; see also Figure S3E), also produced in WT slices by applying the GABA_A antagonist bicuculline (Figures S3B and S3E). Finally, in keeping with input/output data from *Pkr*^{-/-} slices (Figures 2F and 2G), PKRi had no effect on the afferent volley and the initial slope of field EPSPs in WT slices (Figure S3F), but it enhanced population spikes (Figure S3G), as expected if pyramidal neurons were more excitable owing to reduced ongoing inhibition. As expected, PKRi had no effect on population spikes in *Pkr*^{-/-} slices, where PKRi's target (PKR) is absent (Figure S3H) or when inhibition was already blocked (Figure S3I).

PKR acts selectively on GABAergic inhibition, as neither the amplitude nor the frequency of spontaneous excitatory postsynaptic currents (sEPSCs), miniature EPSCs (mEPSCs), or evoked EPSCs (eEPSCs) was significantly changed in PKR deficient

slices (Figure 4). On the basis of our genetic and pharmacological evidence, we conclude that PKR's normal function is to maintain a relatively low level of excitability by enhancing GABAergic synaptic transmission.

Deficient PKR Kinase Activity Facilitates L-LTP

Because the induction of long-term potentiation (LTP) is facilitated by a decrease in GABA tone (Abraham et al., 1986; Davies et al., 1991; Wigström and Gustafsson, 1983), we wondered whether reduced synaptic inhibition in *Pkr*^{-/-} slices (or WT slices treated with PKRi) could facilitate the induction of LTP. Early LTP (E-LTP), typically induced by a single train of high-frequency (tetanic) stimulation, lasts only 1–2 hr and depends on modification of pre-existing proteins, whereas late LTP (L-LTP), generally induced by several (typically four) tetanic trains separated by 5–10 min, persists for many hours and requires new protein synthesis (Kandel, 2001). In WT slices, a single high-frequency stimulus train (100 Hz for 1 s) elicited only a short-lasting E-LTP (Figure 5A). By contrast, in *Pkr*^{-/-} slices, the same stimulation generated a long-lasting late LTP (L-LTP) (Figure 5A), which was blocked by the protein synthesis inhibitor anisomycin (Figure 5B). Four tetanic trains (at 100 Hz) elicited a similar L-LTP in WT and *Pkr*^{-/-} slices (Figure 5C). In agreement with the findings in *Pkr*^{-/-} slices, incubation with PKRi converted a transient E-LTP into a sustained L-LTP in WT slices (Figure 5D) but did not induce any further potentiation in *Pkr*^{-/-} slices (Figure 5E), confirming the specificity of PKRi. These data demonstrate that genetic deletion or pharmacological inhibition of PKR lowers the threshold for the induction of L-LTP.

If L-LTP is facilitated in *Pkr*^{-/-} slices due to reduced inhibition, then reinforcing GABAergic tone should convert the effect of a single train from long-lasting to short-lasting. Indeed, incubation with a low concentration of diazepam (1 μM), which potentiates GABA_A action (Haefely, 1990), markedly reduced L-LTP in *Pkr*^{-/-} slices (Figure 5F) but had no effect on L-LTP induced by four tetanic trains in WT slices (Figure 5G). Only a very high concentration of diazepam (50 μM) reduced L-LTP in WT slices (Figure 5H). These data support our hypothesis that the facilitation of L-LTP in *Pkr*^{-/-} slices is a consequence of decreased GABAergic tone.

Deficient PKR Kinase Activity Enhances Learning and Memory

GABAergic function is crucial for memory consolidation (Izquierdo and Medina, 1991; McGaugh and Roozendaal, 2009). To address whether learning and memory are enhanced in *Pkr*^{-/-} mice, which exhibit impaired hippocampal GABA-mediated inhibition, mice were tested for hippocampus-dependent spatial memory in the Morris water maze (Morris et al., 1982). Because weak tetanic stimulation (one train at 100 Hz) induced L-LTP in slices from *Pkr*^{-/-} mice, we trained mice using a weak protocol (only one training session per day) for 8 days. *Pkr*^{-/-} mice found the platform significantly faster than did WT control littermates (Figure 6A); and in the probe test, performed on day 9, when the platform was removed, only *Pkr*^{-/-} mice remembered the platform location (target quadrant; Figure 6B). Thus, genetic deletion of PKR strengthened spatial LTM.

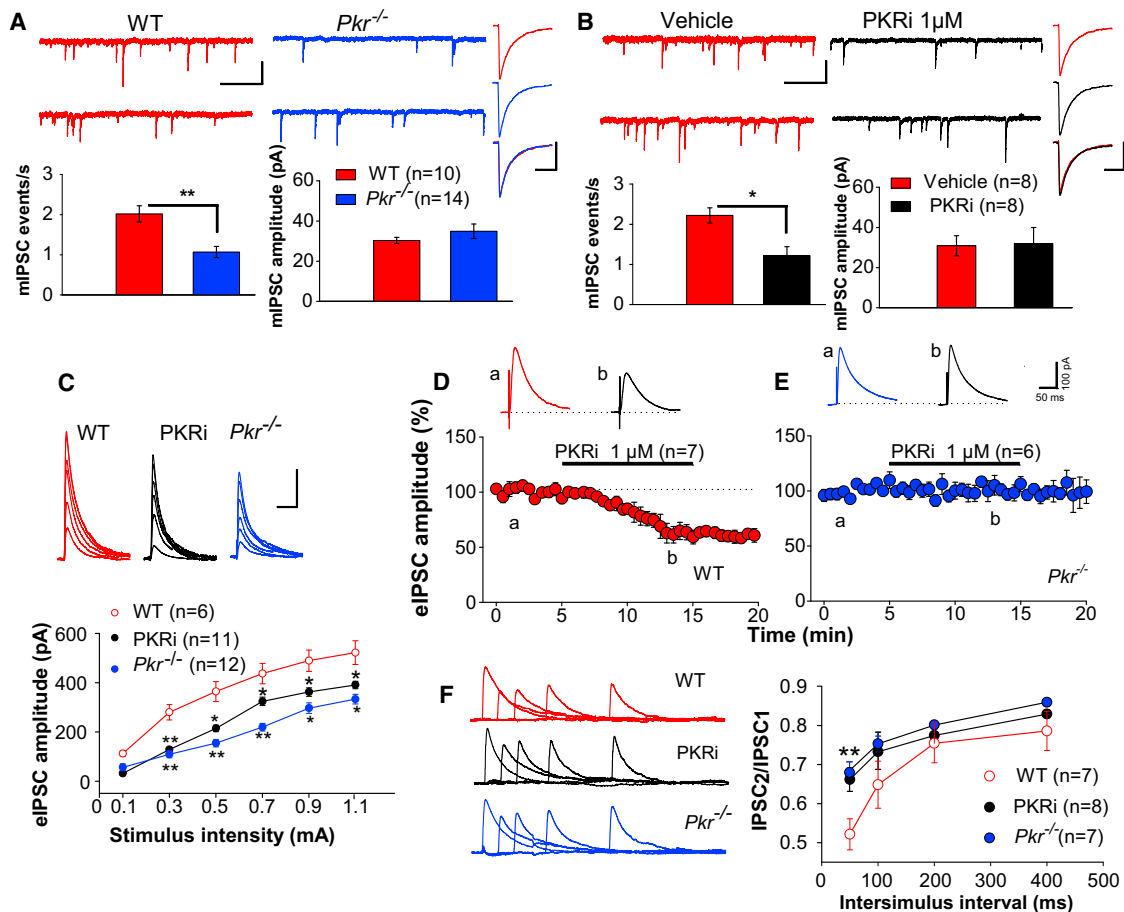


Figure 3. Reduced Inhibitory Synaptic Responses in CA1 of *Pkr*^{-/-} Slices or WT Slices Treated with PKRi

(A) Sample traces (top) and summary data (bottom) show reduced frequency ($t = 4.7$; $**p < 0.01$) but no change in the amplitude (Mann-Whitney U test, $U = 66.0$; $p = 0.84$) of mIPSCs (recorded at -60 mV with a KCl-containing patch pipette and in the presence of the wide-spectrum glutamate antagonist kynurenic acid [2 mM] and tetrodotoxin [TTX, 1 μ M]) in CA1 neurons from *Pkr*^{-/-} mice. Traces at right (each is an average of at least 100 mIPSCs) do not differ between WT (uppermost) and *Pkr*^{-/-} slices (middle), as confirmed by superimposed traces (lowest).

(B) Similarly, in WT slices, PKRi decreased the frequency of mIPSCs ($t = 3.42$; $*p < 0.05$), but not their amplitude ($t = 0.46$; $p = 0.65$). Summary data and individual events are as in (A).

(A and B) Calibrations: 1 s and 50 pA for slow traces; 20 ms and 20 pA for fast traces.

(C) eIPSC amplitude as a function of stimulation intensity is shown superimposed and plotted (below) as input/output curves (recorded at 0 mV in the presence of APV [50 μ M], CNQX [10 μ M], and CGP55845 [10 μ M]) ($*p < 0.05$; $**p < 0.01$). Calibrations: 50 ms and 200 pA.

(D and E) PKRi reduced the amplitude of evoked IPSCs in WT slices (D) ($t = 3.2$; $p < 0.01$), but not in *Pkr*^{-/-} slices (E) (Mann-Whitney U test, $U = 20.2$; $p = 0.62$). Horizontal bar indicates PKRi application. Inset traces were obtained at times "a" and "b."

(F) Paired IPSCs at 50, 100, 200, and 400 ms interstimulus intervals (ISIs) are superimposed (at left) after subtracting the first IPSC from paired responses. Corresponding ratios of IPSC₂/IPSC₁ are plotted at right. Note the reduced paired-pulse depression at 50 ms in *Pkr*^{-/-} slices ($t = 7.85$; $**p < 0.01$) and WT slices treated with PKRi ($t = 3.47$; $**p < 0.01$).

See Figure S2 for further information about sIPSCs and eIPSCs in PKR-deficient slices; Figure S3 for the role of PKR in cumulative GABAergic inhibition; Figure S6A for the reduced mIPSCs in slices from eIF2 α ^{+SS1A} mice; and Figure S7C for the effect of PKRi in vitro.

Mice were also studied in two forms of Pavlovian fear conditioning. Contextual fear conditioning was induced by pairing a context (conditioned stimulus [CS]) with a foot shock (the unconditioned stimulus [US]), whereas in auditory fear conditioning, the US was paired with a tone presentation (CS). Contextual fear conditioning involves both the hippocampus and amygdala, whereas auditory fear conditioning requires only the amygdala (LeDoux, 2000). When mice were subsequently exposed to the same CS, fear responses (freezing) were taken

as an index of the strength of the CS-US association. Naive WT and *Pkr*^{-/-} mice showed a similar amount of freezing prior to a weak training protocol (a single pairing of a tone with a 0.35 mA foot shock), whereas *Pkr*^{-/-} mice exhibited more freezing than did WT control littermates when tested 24 hr later (Figure 6C). Similarly, *Pkr*^{-/-} mice showed enhanced long-term auditory fear memory (Figure 6D). A nonspecific response to fear in *Pkr*^{-/-} mice was unlikely because both baseline freezing (Figures 6C and 6D) and anxiety-reflecting behavior (in the elevated plus

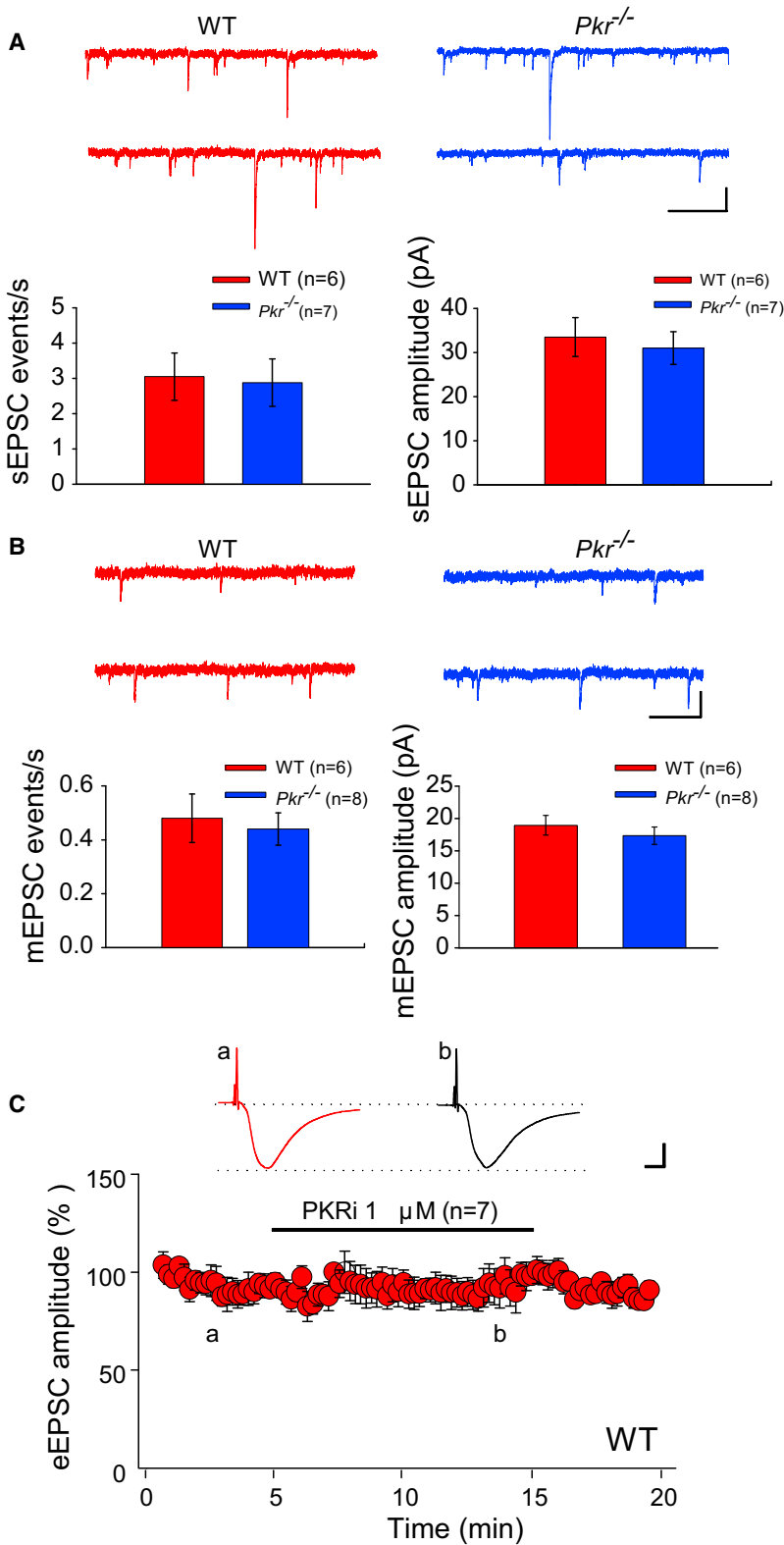


Figure 4. Excitatory Synaptic Transmission Is Unaltered in *Pkr*^{-/-} Slices or WT Slices Treated with PKRi

(A) Whole-cell recordings of EPSCs were performed with gluconate-containing pipettes at -70 mV in the presence of $100 \mu\text{M}$ picrotoxin. Sample traces (top) and summary data (bottom) show similar frequency (Mann-Whitney U test, $U = 20.5$; $p = 0.95$) and amplitude ($t = 0.48$; $p = 0.64$) of spontaneous EPSCs (sEPSCs) in WT and *Pkr*^{-/-} slices. (B) Sample traces (top) and summary data (bottom) show similar frequency (Mann-Whitney U test, $U = 16.2$; $p = 0.34$) and amplitude ($t = 0.34$; $p = 0.74$) of miniature EPSCs (mEPSCs) (recorded in the presence of picrotoxin [$100 \mu\text{M}$] and TTX [$1 \mu\text{M}$]) in WT and *Pkr*^{-/-} slices. (C) PKRi ($1 \mu\text{M}$) had no effect on EPSCs evoked (for “a” versus “b”; illustrated by inset traces, $t = 0.40$; $p = 0.69$) in the presence of $100 \mu\text{M}$ picrotoxin. Horizontal bar indicates the period of incubation with PKRi. (A and B) Calibrations: 1 s and 20 pA. (C) Calibrations: 10 ms and 100 pA. For information about the effect of PKRi in vitro, see Figure S7C.

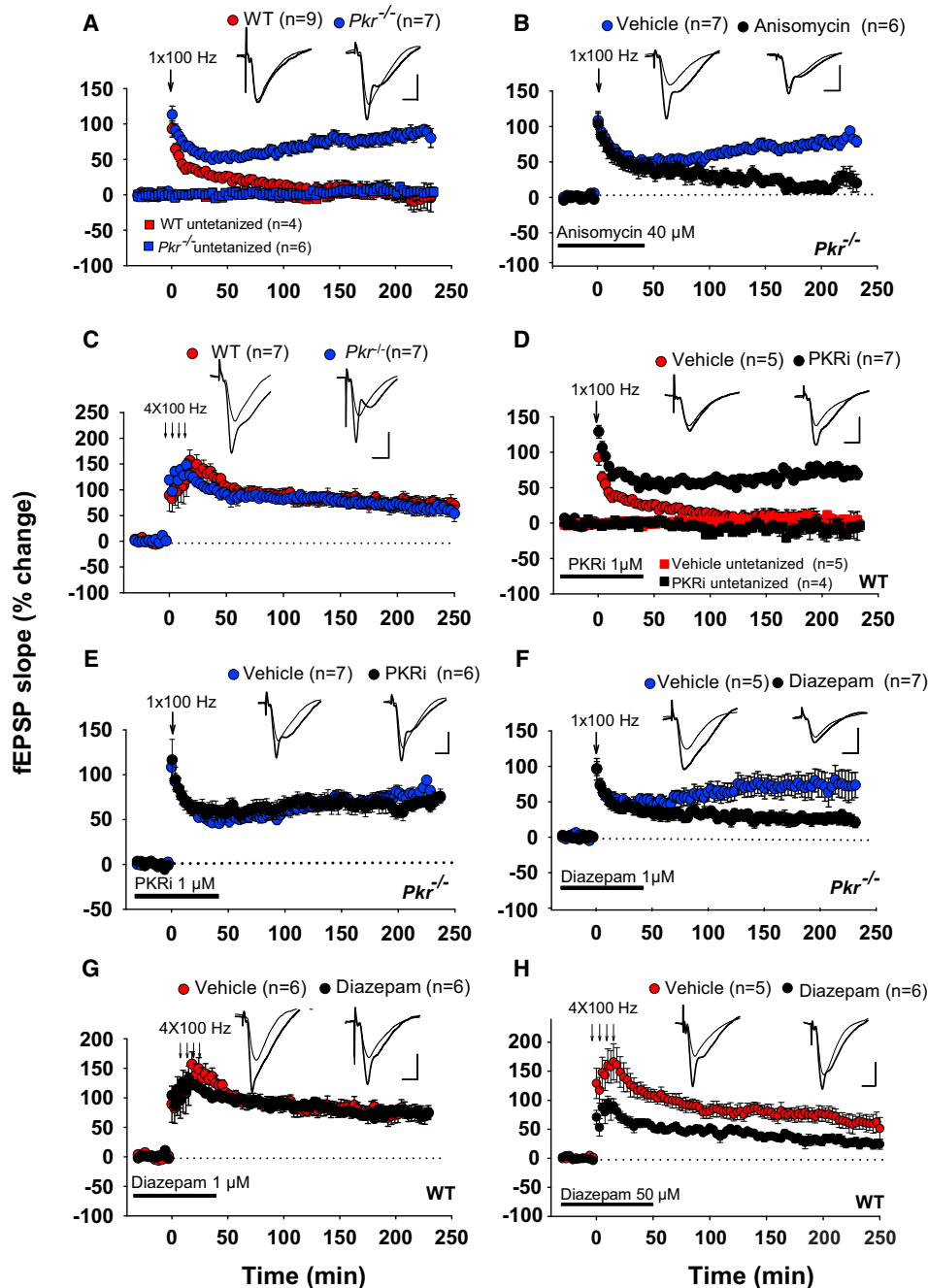


Figure 5. Facilitated L-LTP in *Pkr*^{-/-} Slices or WT Slices Treated with PKRi

(A) A single high-frequency train (100 Hz for 1 s) elicited a short-lasting early LTP (E-LTP) in WT slices but generated a sustained late LTP (L-LTP) in *Pkr*^{-/-} slices ($F_{(1,14)} = 76.8$; $p < 0.001$).

(B) The facilitated L-LTP in *Pkr*^{-/-} slices was suppressed by anisomycin ($F_{(1,11)} = 22.2$; $p < 0.001$).

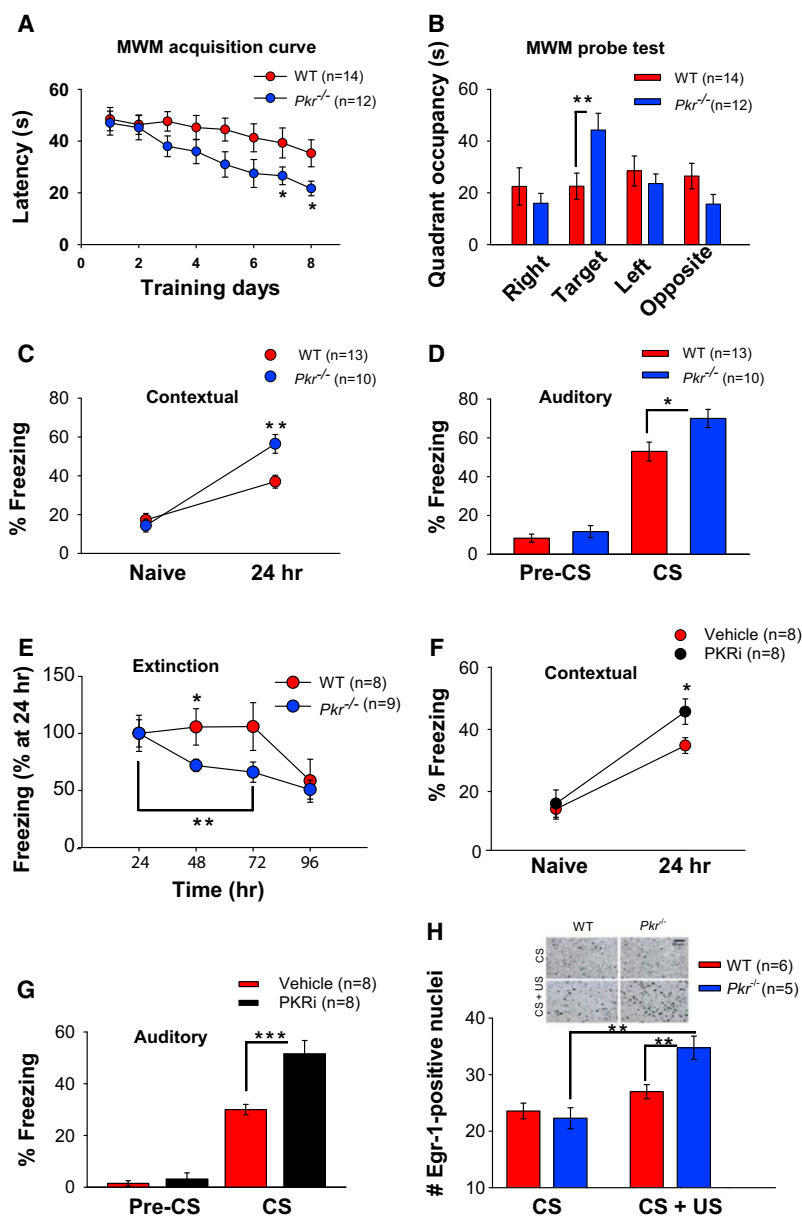
(C) L-LTP induced by four tetanic trains at 100 Hz is similar in WT and *Pkr*^{-/-} slices ($F_{(1,12)} = 0.48$; $p = 0.49$).

(D and E) PKRi converted E-LTP into L-LTP in WT slices (D) ($F_{(1,10)} = 61.2$; $p < 0.001$) but in *Pkr*^{-/-} slices (E) did not further potentiate the sustained LTP elicited by a single high-frequency train ($F_{(1,11)} = 1.1$; $p = 0.18$).

(F and G) A low concentration of diazepam (1 μ M) impaired L-LTP induced by a single tetanus in *Pkr*^{-/-} slices (F) ($F_{(1,10)} = 11.3$; $p < 0.001$), but not the L-LTP induced by four tetani in WT slices (G) ($F_{(1,10)} = 0.23$; $p = 0.64$).

(H) In WT slices, a high concentration of diazepam (50 μ M) impaired L-LTP induction by four trains at 100 Hz ($F_{(1,9)} = 15.4$; $p < 0.01$). Horizontal bars indicate the periods of drug application. (Inset) Superimposed traces obtained before and 220 min after tetanic stimulation. All comparisons were done at 220 min. Calibrations: 5 ms and 3 mV.

For information about the role of PKRi in L-LTP maintenance, see Figure S7A. See Figure S7C for the effect of PKRi in vitro.



maze and open field; Figure S4) were normal in *Pkr*^{-/-} mice. Hence, the lack of PKR improved both auditory and contextual long-term fear memories. Enhanced cognition is also associated with rapid memory extinction (Lee and Silva, 2009) when animals are re-exposed to the same context over several trials but no foot shock is applied. As expected, *Pkr*^{-/-} mice showed faster contextual fear extinction than did WT controls (Figure 6E).

If PKR is involved in cognitive processing, acute pharmacological inhibition of PKR should also potentiate long-term fear memories. To test this prediction, WT mice were injected with either vehicle or PKRi immediately after Pavlovian fear conditioning. Both contextual and auditory long-term fear memories were enhanced in PKRi-treated mice when measured 24 hr after training (Figures 6F and 6G).

Because PKR deficiency enhanced long-term memory storage, we asked whether memory allocation, the process by which neurons or synapses are specifically activated or incorporated in a neural circuit during learning (Silva et al., 2009), is also enhanced in *Pkr*^{-/-} mice. To identify neurons selectively activated during learning, we analyzed the expression of the immediate-early gene *Egr-1* (also called *Zif/268*). *Egr-1* has been extensively used for this purpose (Frankland et al., 2004; Hall et al., 2000), and its deletion blocks L-LTP and memory consolidation (Jones et al., 2001). WT and *Pkr*^{-/-} mice were subjected to a weak fear conditioning protocol (a single pairing of a tone with a 0.35 mA foot shock), and the expression of *Egr-1* in the CA1 region was quantified by immunohistochemistry, as previously described (Frankland et al., 2004). *Egr-1* expression was not significantly different when animals of both genotypes were exposed to the context alone. In contrast, a weak training paradigm, which triggered a more robust long-lasting memory in *Pkr*^{-/-} mice (Figure 6C), increased *Egr-1* levels in CA1 neurons only from *Pkr*^{-/-} mice (Figure 6H). Thus, the lack of PKR favors the recruitment of CA1 neurons into the encoding process.

Figure 6. Enhanced Spatial and Fear Memory in *Pkr*^{-/-} Mice or WT Mice Treated with PKRi

(A) Mean escape latencies as a function of training days in the Morris water maze (one trial/day). Compared to WT controls, escape latencies were significantly shorter for *Pkr*^{-/-} mice after day 6 (day 7, $F_{(1,24)} = 7.4$; day 8, $F_{(1,24)} = 6.4$; * $p < 0.05$).

(B) In the probe test performed on day 9, only *Pkr*^{-/-} mice preferred the target quadrant ($F_{(1,24)} = 11.109$; ** $p < 0.01$).

(C) For contextual fear conditioning, freezing times were recorded before conditioning (naive, during 2 min period) and then 24 hr after training (during 5 min period).

(D) For auditory fear memory, freezing times were measured 24 hr posttraining either before the onset of the tone (pre-CS, for 2 min) or during the tone presentation (for 3 min). Enhanced freezing 24 hr after training indicates stronger fear memory in *Pkr*^{-/-} mice (C, $F_{(1,21)} = 10.2$; ** $p < 0.01$; D, $F_{(1,21)} = 5.2$; * $p < 0.05$).

(E) *Pkr*^{-/-} mice exhibited significantly faster extinction of freezing in response to the context, as compared to WT littermates (at 48 hr, WT versus *Pkr*^{-/-} mice; $F_{(1,15)} = 4.7$; * $p < 0.05$; *Pkr*^{-/-} mice within group, 24–72 hr; $F_{(2,8)} = 12.8$; ** $p < 0.01$).

(F and G) PKRi injection (0.1 mg/kg i.p.) immediately after training enhanced both contextual (F, $F_{(1,14)} = 6.6$; * $p < 0.05$) and auditory (G, $F_{(1,14)} = 19.1$; *** $p < 0.001$) long-term fear memories.

(H) The expression of the immediate-early gene *Egr-1* was similar in CA1 neurons from WT and *Pkr*^{-/-} mice exposed to context (CS). In response to contextual fear training (CS+US), there was a significantly greater number of *Egr-1*-positive neurons in CA1 from *Pkr*^{-/-} mice ($F_{(1,9)} = 11.94$; ** $p < 0.01$; *Pkr*^{-/-} CS versus CS+US, $F_{(1,8)} = 30.7$; ** $p < 0.01$).

For information about the role of PKRi in LTM maintenance, see Figure S7B. See Figure S7D for the effect of PKRi in vivo and Figure S4 for the lack of anxiety-reflecting behavior in *Pkr*^{-/-} mice.

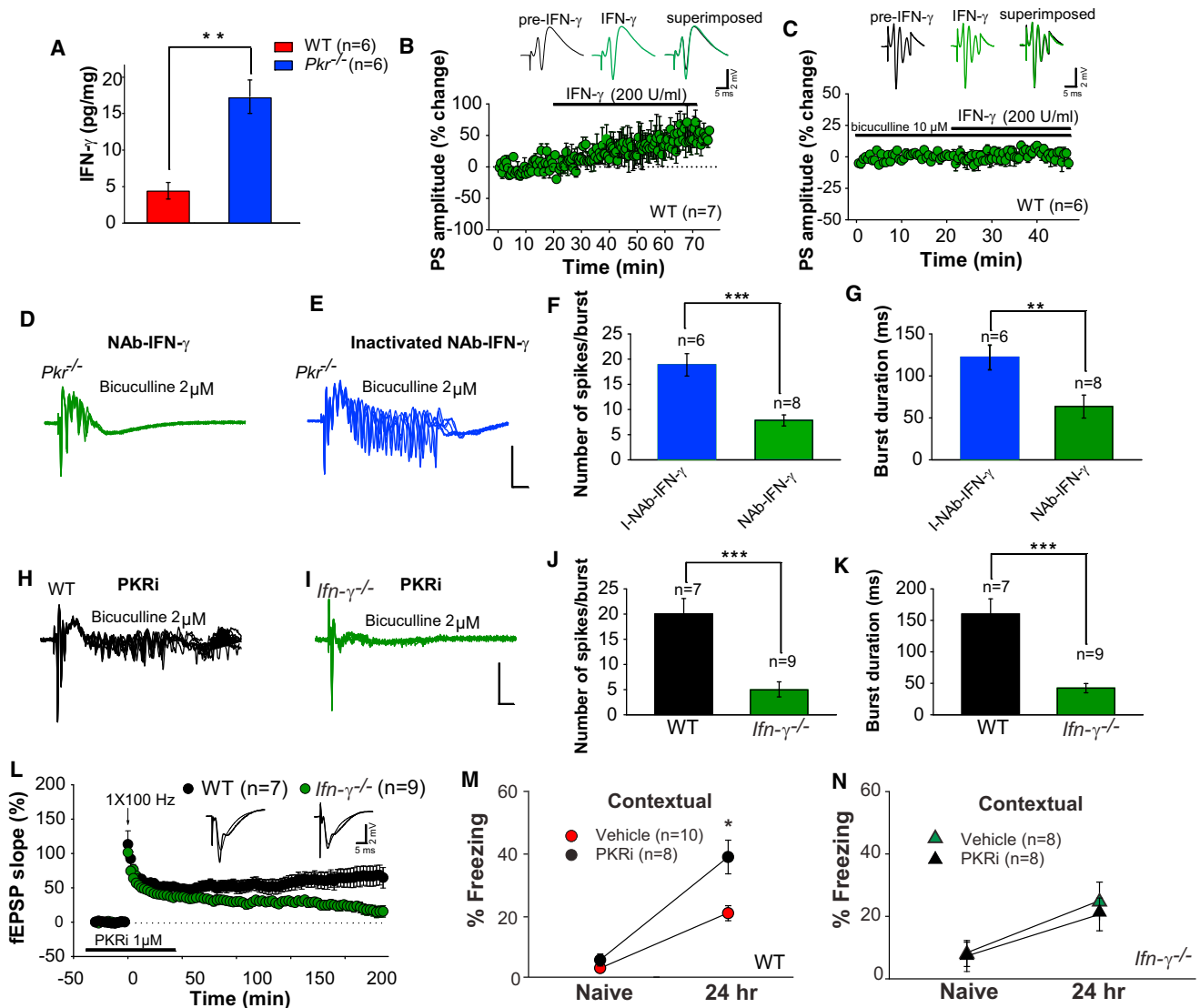


Figure 7. Inhibition of IFN- γ Rescues Hyperexcitability, Facilitated L-LTP, and LTM Caused by PKR Deficiency

(A) IFN- γ was increased in pooled hippocampal extracts from *Pkr*^{-/-} mice (Mann-Whitney U test, $U = 0.00$; ** $p < 0.01$). (B) IFN- γ (200 U/ml) enhanced the amplitude of population spikes in WT slices ($t = 2.65$; $p < 0.05$), but not in the presence of bicuculline (C, $t = 1.03$; $p = 0.33$). (D and E) A neutralizing antibody against IFN- γ (NAb-IFN- γ ; D), but not its heat-inactivated form (E), prevented epileptiform activity enabled by a low concentration of bicuculline (2 μ M) in *Pkr*^{-/-} slices. (F and G) NAb-IFN- γ greatly reduced the number of evoked spikes (F) ($t = 6.52$; *** $p < 0.001$) and burst duration (G) (Mann-Whitney U test, $U = 0.00$, ** $p < 0.01$). (H and I) Combined application of PKRi (1 μ M) with a low concentration of bicuculline (2 μ M) induced prominent after-discharges in WT slices (H), but not in *Ifn*- γ ^{-/-} slices (I). (J and K) Note the great reduction in the number of evoked spikes (J, $t = 6.21$; *** $p < 0.001$) and burst duration (K, $t = 4.21$; *** $p < 0.001$) in *Ifn*- γ ^{-/-} slices. (L) PKRi induced a sustained L-LTP in WT slices, but not in *Ifn*- γ ^{-/-} slices ($F_{(1,14)} = 14.9$; $p < 0.01$). (M and N) Injection of PKRi (0.2 mg/kg i.p.) immediately after training enhanced long-term contextual fear memory in WT mice (M) ($F_{(1,16)} = 6.9$, $p < 0.05$) but had no effect in *Ifn*- γ ^{-/-} mice (N) ($F_{(1,14)} = 0.62$; $p = 0.44$). For further information about IFN- γ and PKRi in hyperexcitability and auditory long-term fear memory, see Figure S5. For information about the effect of PKRi in vitro and in vivo, see Figures S7C and S7D.

Inhibition of Interferon- γ in PKR-Deficient Mice Restores Normal Excitability, LTP, and Memory

Given that IFN- γ increases neuronal excitability in hippocampal slices by reducing GABA release (Müller et al., 1993) and that PKR suppresses the translation of IFN- γ mRNA (Ben-Asouli

et al., 2002; Cohen-Chalamish et al., 2009), we hypothesized that the hyperexcitability of neural networks in PKR-deficient mice might be caused by IFN- γ -mediated disinhibition. In accordance with this prediction, IFN- γ levels were increased in the hippocampus from *Pkr*^{-/-} mice (Figure 7A). Similar to treatment

with PKRi (see Figure S3G), addition of exogenous IFN- γ enhanced the amplitude of CA1 population spikes in WT slices (Figure 7B) but had no effect in slices preincubated with bicuculline (10 μ M), in which GABAergic synaptic transmission was already blocked (Figure 7C), or in those treated with a monoclonal neutralizing antibody against IFN- γ (NAb-IFN- γ ; Figure S5A), which specifically binds to IFN- γ and blocks its biological activity (Buchmeier and Schreiber, 1985; Schreiber et al., 1985).

To test whether inhibition of IFN- γ could restore normal excitability in PKR-deficient slices, we blocked IFN- γ 's function with NAb-IFN- γ . After discharges induced by a low concentration of bicuculline in *Pkr*^{-/-} slices were drastically reduced by bath application of NAb-IFN- γ , but not by a heat-inactivated form of the same antibody (I-NAb-IFN- γ , compare Figure 7D to 7E; see also Figures 7F and 7G). Accordingly, in WT slices, PKRi failed to increase the amplitude of population spikes in the presence of a NAb-IFN- γ (compare Figure S3G to S5B) or the inhibitor of translation anisomycin (compare Figure S3G to S5C). Taken together, these data indicate that the increased excitability in PKR-deficient slices is mediated by endogenous IFN- γ . In contrast to WT slices (Figure 7H; see also Figures 7J and 7K), the combination of PKRi and 2 μ M bicuculline failed to generate epileptiform after-discharges in *Irfn- γ* ^{-/-} slices (Figure 7I; see also Figures 7J and 7K), thus demonstrating that the increased excitability of WT slices induced by PKRi requires IFN- γ . Therefore, two quite independent approaches—genetics (*Irfn- γ* ^{-/-} mice) and immunology (NAb-IFN- γ)—showed that the hyperexcitability of PKR-deficient slices was primarily due to IFN- γ -mediated disinhibition.

To determine whether PKR deficiency facilitates L-LTP and enhances LTM via IFN- γ , *Irfn- γ* ^{-/-} mice and WT mice were treated with PKRi. In contrast to its effect in WT slices, in *Irfn- γ* ^{-/-} slices, PKRi failed to promote L-LTP induced by a single high-frequency train (Figure 7L). Similarly, PKRi enhanced long-term fear memories in WT mice, but not in *Irfn- γ* ^{-/-} mice (Figures 7M, 7N, S5D, and S5E). These data provide evidence that the facilitation of both L-LTP and LTM in PKRi-treated mice is due, at least in part, to IFN- γ -mediated disinhibition.

DISCUSSION

Our data reveal that the lack of a double-stranded RNA-activated protein kinase PKR, originally identified as a sensor of virus infection, unexpectedly leads to hyperexcitability in cortical and hippocampal networks. In addition, L-LTP and behavioral learning are enhanced in *Pkr*^{-/-} mice or when PKR activity is pharmacologically blocked. The increased excitability in PKR-deficient mice is caused by IFN- γ -mediated disinhibition. Thus, PKR regulates network rhythmicity, synaptic plasticity, and memory storage by potentiating GABAergic synaptic transmission.

GABAergic inhibition not only controls the efficacy and plasticity of excitatory synapses, but also promotes the synchronized firing of large assemblies of principal cells at certain preferred frequencies (Mann and Paulsen, 2007). Slow theta and faster gamma oscillations and ripples appear to be crucially involved in mnemonic processes (Buzsaki, 2006; Maurer and

McNaughton, 2007). Multiple lines of evidence support the idea that GABAergic control of synaptic plasticity is a key mechanism of memory storage (Mann and Paulsen, 2007; Paulsen and Moser, 1998). First, reduced GABAergic-mediated inhibition facilitates the induction of LTP (Abraham et al., 1986; Davies et al., 1991; Wigström and Gustafsson, 1983). Second, long-term disinhibition of a subset of CA1 pyramidal neurons correlates with the acquisition of spatial memory (Gusev and Alkon, 2001). Third, modest pharmacological reduction of GABAergic transmission enhances memory consolidation (Izquierdo and Medina, 1991; McGaugh and Roozendaal, 2009). Finally, GABAergic neurons of the medial septum drive theta rhythmicity in the hippocampal network (Hangya et al., 2009).

Our results provide new insight into the function of PKR in the adult brain and how the suppression of PKR promotes network hypersynchrony and enhances L-LTP and cognitive performance. We propose a model in which PKR regulates these processes by IFN- γ -mediated disinhibition. This model is consistent with the following observations. First, IFN- γ increases excitability (Figure 7B) and generates paroxysmal discharges in hippocampal slices by reducing GABA release at inhibitory synapses (Müller et al., 1993). Second, through a pseudoknot in its 5'UTR, IFN- γ mRNA locally activates PKR and eIF2 α to inhibit its own translation, but not translation of other mRNAs (Ben-Asouli et al., 2002; Cohen-Chalamish et al., 2009). Hence, *Irfn- γ* mRNA translation is enhanced when PKR is genetically or pharmacologically inhibited or when eIF2 α phosphorylation is reduced (Ben-Asouli et al., 2002). Accordingly, the levels of IFN- γ were enhanced in the hippocampus (Figure 7A; and possibly also in the amygdala) from *Pkr*^{-/-} mice. Third, in WT slices, PKRi increases neuronal excitability in a translation-dependent manner (Figures S3G and S5C). Fourth, like *Pkr*^{-/-} mice, animals with constitutively reduced eIF2 α phosphorylation (eIF2 α ^{+S51A} mice) showed facilitated L-LTP and LTM (Costa-Mattioli et al., 2007), reduced GABAergic synaptic transmission (Figures S6A and S6B), and EEG synchronous spike discharges (Figures S6C and S6D), supporting the notion that PKR, via the phosphorylation of eIF2 α , regulates translation of *Irfn- γ* mRNA. Fifth, chemically mediated increase in eIF2 α phosphorylation blocks L-LTP and LTM in the murine forebrain (Jiang et al., 2010). Sixth, *Irfn- γ* ^{-/-} mice are resistant to both virus- and kainic acid-induced limbic seizures (Getts et al., 2007). Finally, spatial memory is enhanced in transgenic mice overexpressing small amounts of IFN- γ (Baron et al., 2008). Thus, our observations show that PKR and IFN- γ —both crucial components of the antiviral and inflammatory response (Farrar and Schreiber, 1993; Garcia et al., 2007)—play an important role in activity-dependent changes in synaptic strength and network rhythmicity in the adult brain.

In contrast to PKR, which selectively regulates inhibitory presynaptic terminals and controls the induction of L-LTP and LTM (but not their maintenance; Figures S7A and S7B), protein kinase Mzeta (PKMzeta), which targets excitatory synapses by reconfiguring postsynaptic AMPA receptor trafficking, is a unique factor that is both necessary and sufficient for the maintenance of L-LTP and LTM (Sacktor, 2011). Another well-characterized kinase complex controlling protein synthesis-dependent L-LTP and LTM is the mammalian target of rapamycin complex 1

(mTORC1) (Richter and Klann, 2009; Stoica et al., 2011). However, the nature and the precise synaptic mechanism by which mTORC1-dependent proteins promote L-LTP and LTM remain unknown.

In conclusion, we report here a mouse model in which the lack of the eIF2 α kinase PKR, through IFN- γ -mediated reduction of GABAergic inhibition, results in network hyperexcitability, enhanced long-lasting synaptic plasticity, and improved cognitive performance.

In view of the robust and consistent enhancement in learning and memory produced by loss of PKR or by treatment with PKRi, it is reasonable to suggest that PKRi (or agents which target PKR) may similarly benefit humans, especially those experiencing age-related memory loss or patients suffering from the most devastating memory loss associated with Alzheimer's disease, in which PKR activity is indeed known to be abnormally elevated.

EXPERIMENTAL PROCEDURES

Mice

Pkr knockout (*Pkr*^{-/-}) mice (Abraham et al., 1999) were backcrossed for at least eight generations to 129SvEv mice. eIF2 α ^{+/SS1A} mice have been previously described (Costa-Mattioli et al., 2007). *Irfn- γ* ^{-/-} mice and WT CF57/Bl6 control mice were obtained from Jackson Laboratories. All experiments were performed on 8- to 16-week-old males. Mice were kept on a 12 hr light/dark cycle, and the behavioral experiments were conducted during the light phase of the cycle. Mice had access to food and water ad libitum, except during tests. Animal care and experimental procedures were performed with approval from the animal care committees of Baylor College of Medicine.

Chronic Videoelectroencephalographic Monitoring

Videoelectroencephalographic (VideoEEG) recordings were performed as previously described (Price et al., 2009). *Pkr*^{-/-} mice and WT littermates were anesthetized with Avertin (1.25% tribromoethanol/amyl alcohol solution, i.p.) at a dose of 0.02 ml/g. Teflon-coated silver wire electrodes (120 μ m diameter) soldered to a microminiature connector were implanted bilaterally into the subdural space over frontal, central, parietal, and occipital cortices and 2.0 mm deep into the dorsal hippocampus bilaterally. All recordings were done at least 24 hr after surgery on mice freely moving in the test cage. Digitized videoEEG data were obtained daily for up to 2 weeks during prolonged and random 2 hr sample recordings (Stellate Systems, Harmonie software version 5.0b). The EEG data were interpreted by two experienced mouse electrocorticographers blinded to genotype, and interictal spikes (100–300 μ V, 20–100 ms duration) and seizure frequency were included for analysis.

Electrophysiology

All electrophysiology experiments were done by investigators blind to the genotype. Field recordings were from CA1 in horizontal hippocampal slices (350 μ m), maintained at 28°C–29°C in interface chamber, as previously described (Costa-Mattioli et al., 2007; Stoica et al., 2011); for additional information, see [Extended Experimental Procedures](#). Whole-cell recordings were performed at 28°C–29°C using conventional patch-clamp techniques and an Axopatch 200B amplifier (Molecular Devices, Union City, CA). CA1 neurons were visually identified by infrared differential interference contrast video microscopy on the stage of an upright microscope (Axioskope FS2, Carl Zeiss, Oberkochen, Germany). Patch pipettes (resistances 4–6 M Ω) were filled with (in mM): 110 K-gluconate, 10 KCl, 10 HEPES, 10 Na₂-phosphocreatine, 2 Mg₃-ATP, and 0.2 Na₃-GTP; pH was adjusted to 7.2 and osmolarity to 290 mOsm using a Wescor 5500 vapor pressure osmometer (Wescor, Logan, UT). Synaptic responses were evoked with a bipolar stimulating electrode positioned in stratum radiatum. For recording of inhibitory synaptic currents, gluconate was replaced with KCl. sIPSCs were recorded in the presence of 2 mM kynurenic acid, and miniature IPSCs (mIPSCs) were recorded in

the presence of kynurenic acid (2 mM) and tetrodotoxin (TTX; 1 μ M). Evoked IPSCs were recorded in the presence or absence of D-AP5 (50 μ M), CNQX (10 μ M), and CGP55845 (10 μ M). Excitatory postsynaptic currents (EPSCs) were recorded in the presence of 10 μ M bicuculline or 100 μ M picrotoxin. All synaptic events were sampled 10–15 min after washing in PKRi. The electrical signals were filtered online at 5 kHz and digitized at 10 kHz. Series and input resistance were measured continually during recording by injecting a –5 mV \times 25 ms test pulse prior to stimulus. If they varied more than \pm 20%, recording was abandoned and the data were discarded. All drugs were obtained from Tocris (Ellisville, MO) (unless otherwise indicated).

Contextual and Auditory Fear Conditioning

The investigators were blind to the genotype for all behavioral tests. Fear conditioning was performed as previously described (Costa-Mattioli et al., 2007; Stoica et al., 2011). Mice were first handled for 3–5 min for 3 days and then habituated to the conditioning chamber for 20 min for another 3 days. On the training day, after 2 min in the conditioning chamber, mice received a pairing of a tone (2800 Hz, 85 db, 30 s) with a coterminating foot shock (0.35 mA, 1 s), after which they remained in the chamber for 2 additional min and were then returned to their home cages. Mice were tested 24 hr after training for “freezing” (immobility with the exception of respiration) in response to the tone (in a chamber to which they had not been conditioned) and to the training context (training chamber).

During testing for auditory fear conditioning, mice were placed in the chamber and freezing responses were recorded during the initial 2 min (pre-CS period) and during the last 3 min when the tone was played (CS period). Mice were returned to their cages 30 s after the end of the tone. For tests of contextual fear conditioning, mice were returned to the conditioning chamber for 5 min. Tests of responses to the training context (chamber A) and to the tone (chamber B) were done in a counterbalanced manner. Extinction was studied in a different set of animals, and freezing in response to the conditioned context was assessed for 5 min at 24 hr, 48 hr, 72 hr, and 96 hr after training and normalized to the amount of freezing obtained at 24 hr. For all tests, freezing behavior was hand scored at 5 s intervals during the 5 min period by a rater who was blind to the genotype. The percent of time spent by the mouse freezing was taken as an index of learning and memory. PKRi was freshly dissolved in saline and then i.p. injected immediately after fear conditioning at a dose of 0.1 mg/kg, which is known to block PKR activity in the hippocampus in vivo (Ingrand et al., 2007; for additional information, see [Extended Experimental Procedures](#)).

Morris Water Maze

In a circular pool (140 cm diameter) of opaque water (kept at 22°C–23°C), WT and *Pkr*^{-/-} littermates were trained daily for 8 days using a relatively weak training protocol, one trial per day (Costa-Mattioli et al., 2007). The latencies of escape from the water onto the hidden (submerged) platform (10 cm of diameter) were monitored by an automated video tracking system (HVS Image, Buckingham, UK). For the probe trial, which was performed on day 9, the platform was removed from the pool and the animals were allowed to search for 60 s. The percentage of time spent in each quadrant of the pool (quadrant occupancy) was recorded. There was no significant difference in swimming speed between *Pkr*^{-/-} mice and WT littermates (16.9 \pm 0.87 cm/s for WT and 16.3 \pm 0.7 cm/s for *Pkr*^{-/-} mice, $F_{(1,24)} = 0.27$, $p = 0.61$). The animals were trained at the same time of day during their light phase.

Immunohistochemistry, Western Blotting, and ELISA

For all immunohistochemical experiments, the investigators were blind to the genotype. Hippocampal cell lysates, western blotting, and immunohistochemistry were performed as previously described (Costa-Mattioli et al., 2007; Stoica et al., 2011).

Statistical Analyses

All data are presented as means \pm SEMs. The statistics were based on Student's *t* test or one-way ANOVA and between group comparisons by Tukey's Test, unless otherwise indicated. $p < 0.05$ was considered significant. * $p < 0.05$, ** $p < 0.01$, and *** $p < 0.001$.

SUPPLEMENTAL INFORMATION

Supplemental Information includes Extended Experimental Procedures, seven figures, one table, and one movie and can be found with this article online at doi:10.1016/j.cell.2011.11.029.

ACKNOWLEDGMENTS

We thank G. Buzsáki, H. Zoghbi, and M. Rasband for comments on an early version of the manuscript. This work was supported by funds to M.C.-M. (Searle award 09-SSP-211; George and Cynthia Mitchell Foundation, Baylor IDDRC), J.L.N. (NINDS NS 29709, NICHD HD24064, Baylor IDDRC), and M.J.F. (NEI EY12782). The authors declare no competing financial interests.

Received: June 7, 2011

Revised: September 6, 2011

Accepted: November 2, 2011

Published: December 8, 2011

REFERENCES

- Abraham, W.C., Gustafsson, B., and Wigström, H. (1986). Single high strength afferent volleys can produce long-term potentiation in the hippocampus in vitro. *Neurosci. Lett.* **70**, 217–222.
- Abraham, N., Stojdl, D.F., Duncan, P.L., Méthot, N., Ishii, T., Dubé, M., Vanderhyden, B.C., Atkins, H.L., Gray, D.A., McBurney, M.W., et al. (1999). Characterization of transgenic mice with targeted disruption of the catalytic domain of the double-stranded RNA-dependent protein kinase, PKR. *J. Biol. Chem.* **274**, 5953–5962.
- Bando, Y., Onuki, R., Katayama, T., Manabe, T., Kudo, T., Taira, K., and Tohyama, M. (2005). Double-strand RNA dependent protein kinase (PKR) is involved in the extrastriatal degeneration in Parkinson's disease and Huntington's disease. *Neurochem. Int.* **46**, 11–18.
- Baron, R., Nemirovsky, A., Harpaz, I., Cohen, H., Owens, T., and Monsonego, A. (2008). IFN-gamma enhances neurogenesis in wild-type mice and in a mouse model of Alzheimer's disease. *FASEB J.* **22**, 2843–2852.
- Beenhakker, M.P., and Huguenard, J.R. (2009). Neurons that fire together also conspire together: is normal sleep circuitry hijacked to generate epilepsy? *Neuron* **62**, 612–632.
- Ben-Asouli, Y., Banai, Y., Pel-Or, Y., Shir, A., and Kaempfer, R. (2002). Human interferon-gamma mRNA autoregulates its translation through a pseudoknot that activates the interferon-inducible protein kinase PKR. *Cell* **108**, 221–232.
- Buchmeier, N.A., and Schreiber, R.D. (1985). Requirement of endogenous interferon-gamma production for resolution of *Listeria monocytogenes* infection. *Proc. Natl. Acad. Sci. USA* **82**, 7404–7408.
- Buzsáki, G. (2006). *Rhythms of the Brain* (New York: Oxford University Press).
- Carnevali, L.S., Pereira, C.M., Jaqueta, C.B., Alves, V.S., Paiva, V.N., Vattem, K.M., Wek, R.C., Mello, L.E., and Castilho, B.A. (2006). Phosphorylation of the alpha subunit of translation initiation factor-2 by PKR mediates protein synthesis inhibition in the mouse brain during status epilepticus. *Biochem. J.* **397**, 187–194.
- Chavez-Noriega, L.E., Bliss, T.V., and Halliwell, J.V. (1989). The EPSP-spike (E-S) component of long-term potentiation in the rat hippocampal slice is modulated by GABAergic but not cholinergic mechanisms. *Neurosci. Lett.* **104**, 58–64.
- Cohen-Chalamish, S., Hasson, A., Weinberg, D., Namer, L.S., Banai, Y., Osman, F., and Kaempfer, R. (2009). Dynamic refolding of IFN-gamma mRNA enables it to function as PKR activator and translation template. *Nat. Chem. Biol.* **5**, 896–903.
- Cossart, R., Bernard, C., and Ben-Ari, Y. (2005). Multiple facets of GABAergic neurons and synapses: multiple fates of GABA signalling in epilepsies. *Trends Neurosci.* **28**, 108–115.
- Costa-Mattioli, M., Gobert, D., Stern, E., Gamache, K., Colina, R., Cuello, C., Sossin, W., Kaufman, R., Pelletier, J., Rosenblum, K., et al. (2007). eIF2alpha phosphorylation bidirectionally regulates the switch from short- to long-term synaptic plasticity and memory. *Cell* **129**, 195–206.
- Couturier, J., Morel, M., Pontcharraud, R., Gontier, V., Fauconneau, B., Paccalin, M., and Page, G. (2010). Interaction of double-stranded RNA-dependent protein kinase (PKR) with the death receptor signaling pathway in amyloid beta (Aβ)-treated cells and in APPSLPS1 knock-in mice. *J. Biol. Chem.* **285**, 1272–1282.
- Davies, C.H., Starkey, S.J., Pozza, M.F., and Collingridge, G.L. (1991). GABA autoreceptors regulate the induction of LTP. *Nature* **349**, 609–611.
- Dever, T.E., Dar, A.C., and Sicheri, F. (2007). The eIF2alpha kinases. In *Translational Control in Biology and Medicine*, M.B. Mathews, N. Sonenberg, and J.W.B. Hershey, eds. (Cold Spring Harbor, NY: Cold Spring Harbor Laboratory Press), pp. 319–345.
- Farrar, M.A., and Schreiber, R.D. (1993). The molecular cell biology of interferon-gamma and its receptor. *Annu. Rev. Immunol.* **11**, 571–611.
- Frankland, P.W., Bontempi, B., Talton, L.E., Kaczmarek, L., and Silva, A.J. (2004). The involvement of the anterior cingulate cortex in remote contextual fear memory. *Science* **304**, 881–883.
- Freund, T.F. (2003). Interneuron Diversity series: Rhythm and mood in perisomatic inhibition. *Trends Neurosci.* **26**, 489–495.
- García, M.A., Meurs, E.F., and Esteban, M. (2007). The dsRNA protein kinase PKR: virus and cell control. *Biochimie* **89**, 799–811.
- Getts, D.R., Matsumoto, I., Müller, M., Getts, M.T., Radford, J., Shrestha, B., Campbell, I.L., and King, N.J. (2007). Role of IFN-gamma in an experimental murine model of West Nile virus-induced seizures. *J. Neurochem.* **103**, 1019–1030.
- Girardeau, G., Benchenane, K., Wiener, S.I., Buzsáki, G., and Zugaro, M.B. (2009). Selective suppression of hippocampal ripples impairs spatial memory. *Nat. Neurosci.* **12**, 1222–1223.
- Gusev, P.A., and Alkon, D.L. (2001). Intracellular correlates of spatial memory acquisition in hippocampal slices: long-term disinhibition of CA1 pyramidal cells. *J. Neurophysiol.* **86**, 881–899.
- Haefely, W. (1990). The GABA-benzodiazepine interaction fifteen years later. *Neurochem. Res.* **15**, 169–174.
- Hall, J., Thomas, K.L., and Everitt, B.J. (2000). Rapid and selective induction of BDNF expression in the hippocampus during contextual learning. *Nat. Neurosci.* **3**, 533–535.
- Hangya, B., Borhegyi, Z., Szilágyi, N., Freund, T.F., and Varga, V. (2009). GABAergic neurons of the medial septum lead the hippocampal network during theta activity. *J. Neurosci.* **29**, 8094–8102.
- Heaton, P., and Wallace, G.L. (2004). Annotation: the savant syndrome. *J. Child Psychol. Psychiatry* **45**, 899–911.
- Holmes, G.L., and Lenck-Santini, P.P. (2006). Role of interictal epileptiform abnormalities in cognitive impairment. *Epilepsy Behav.* **8**, 504–515.
- Hughes, J.R. (2010). A review of Savant Syndrome and its possible relationship to epilepsy. *Epilepsy Behav.* **17**, 147–152.
- Huguenard, J.R., and McCormick, D.A. (2007). Thalamic synchrony and dynamic regulation of global forebrain oscillations. *Trends Neurosci.* **30**, 350–356.
- Ingrand, S., Barrier, L., Lafay-Chebassier, C., Fauconneau, B., Page, G., and Hugon, J. (2007). The oxindole/imidazole derivative C16 reduces in vivo brain PKR activation. *FEBS Lett.* **581**, 4473–4478.
- Izquierdo, I., and Medina, J.H. (1991). GABAA receptor modulation of memory: the role of endogenous benzodiazepines. *Trends Pharmacol. Sci.* **12**, 260–265.
- Jammi, N.V., Whitby, L.R., and Beal, P.A. (2003). Small molecule inhibitors of the RNA-dependent protein kinase. *Biochem. Biophys. Res. Commun.* **308**, 50–57.
- Jiang, Z., Belforte, J.E., Lu, Y., Yabe, Y., Pickel, J., Smith, C.B., Je, H.S., Lu, B., and Nakazawa, K. (2010). eIF2alpha Phosphorylation-dependent translation in CA1 pyramidal cells impairs hippocampal memory consolidation without affecting general translation. *J. Neurosci.* **30**, 2582–2594.

- Jones, M.W., Errington, M.L., French, P.J., Fine, A., Bliss, T.V., Garel, S., Charnay, P., Bozon, B., Laroche, S., and Davis, S. (2001). A requirement for the immediate early gene *Zif268* in the expression of late LTP and long-term memories. *Nat. Neurosci.* *4*, 289–296.
- Kandel, E.R. (2001). The molecular biology of memory storage: a dialogue between genes and synapses. *Science* *294*, 1030–1038.
- Klausberger, T., and Somogyi, P. (2008). Neuronal diversity and temporal dynamics: the unity of hippocampal circuit operations. *Science* *321*, 53–57.
- LeDoux, J.E. (2000). Emotion circuits in the brain. *Annu. Rev. Neurosci.* *23*, 155–184.
- Lee, Y.S., and Silva, A.J. (2009). The molecular and cellular biology of enhanced cognition. *Nat. Rev. Neurosci.* *10*, 126–140.
- Mann, E.O., and Paulsen, O. (2007). Role of GABAergic inhibition in hippocampal network oscillations. *Trends Neurosci.* *30*, 343–349.
- Mann, E.O., and Mody, I. (2010). Control of hippocampal gamma oscillation frequency by tonic inhibition and excitation of interneurons. *Nat. Neurosci.* *13*, 205–212.
- Maurer, A.P., and McNaughton, B.L. (2007). Network and intrinsic cellular mechanisms underlying theta phase precession of hippocampal neurons. *Trends Neurosci.* *30*, 325–333.
- McGaugh, J.L., and Roozendaal, B. (2009). Drug enhancement of memory consolidation: historical perspective and neurobiological implications. *Psychopharmacology (Berl.)* *202*, 3–14.
- Morris, R.G., Garrud, P., Rawlins, J.N., and O'Keefe, J. (1982). Place navigation impaired in rats with hippocampal lesions. *Nature* *297*, 681–683.
- Müller, M., Fontana, A., Zbinden, G., and Gähwiler, B.H. (1993). Effects of interferons and hydrogen peroxide on CA3 pyramidal cells in rat hippocampal slice cultures. *Brain Res.* *619*, 157–162.
- Noebels, J.L. (2003). The biology of epilepsy genes. *Annu. Rev. Neurosci.* *26*, 599–625.
- Paquet, C., Bose, A., Polivka, M., Peoc'h, K., Brouland, J.P., Keohane, C., Hugon, J., and Gray, F. (2009). Neuronal phosphorylated RNA-dependent protein kinase in Creutzfeldt-Jakob disease. *J. Neuropathol. Exp. Neurol.* *68*, 190–198.
- Paulsen, O., and Moser, E.I. (1998). A model of hippocampal memory encoding and retrieval: GABAergic control of synaptic plasticity. *Trends Neurosci.* *21*, 273–278.
- Peel, A.L., and Bredesen, D.E. (2003). Activation of the cell stress kinase PKR in Alzheimer's disease and human amyloid precursor protein transgenic mice. *Neurobiol. Dis.* *14*, 52–62.
- Peel, A.L., Rao, R.V., Cottrell, B.A., Hayden, M.R., Ellerby, L.M., and Bredesen, D.E. (2001). Double-stranded RNA-dependent protein kinase, PKR, binds preferentially to Huntington's disease (HD) transcripts and is activated in HD tissue. *Hum. Mol. Genet.* *10*, 1531–1538.
- Price, M.G., Yoo, J.W., Burgess, D.L., Deng, F., Hrachovy, R.A., Frost, J.D., Jr., and Noebels, J.L. (2009). A triplet repeat expansion genetic mouse model of infantile spasms syndrome, *Arx(GCG)10+7*, with interneuronopathy, spasms in infancy, persistent seizures, and adult cognitive and behavioral impairment. *J. Neurosci.* *29*, 8752–8763.
- Richter, J.D., and Klann, E. (2009). Making synaptic plasticity and memory last: mechanisms of translational regulation. *Genes Dev.* *23*, 1–11.
- Sacktor, T.C. (2011). How does PKM ζ maintain long-term memory? *Nat. Rev. Neurosci.* *12*, 9–15.
- Schreiber, R.D., Hicks, L.J., Celada, A., Buchmeier, N.A., and Gray, P.W. (1985). Monoclonal antibodies to murine gamma-interferon which differentially modulate macrophage activation and antiviral activity. *J. Immunol.* *134*, 1609–1618.
- Silva, A.J., Zhou, Y., Rogerson, T., Shobe, J., and Balaji, J. (2009). Molecular and cellular approaches to memory allocation in neural circuits. *Science* *326*, 391–395.
- Sohal, V.S., Zhang, F., Yizhar, O., and Deisseroth, K. (2009). Parvalbumin neurons and gamma rhythms enhance cortical circuit performance. *Nature* *459*, 698–702.
- Steriade, M. (2005). Cellular substrates of brain rhythms. In *Electroencephalography: Basic Principles, Clinical Application, And Related Fields*, E.F.L.D.S. Niedermeyer, ed. (Philadelphia: Lippincott Williams and Wilkins), pp. 505–621.
- Stoica, L., Zhu, P.J., Huang, W., Zhou, H., Kozma, S.C., and Costa-Mattioli, M. (2011). Selective pharmacogenetic inhibition of mammalian target of Rapamycin complex I (mTORC1) blocks long-term synaptic plasticity and memory storage. *Proc. Natl. Acad. Sci. USA* *108*, 3791–3796.
- Thomson, A.M. (2000). Facilitation, augmentation and potentiation at central synapses. *Trends Neurosci.* *23*, 305–312.
- Wigström, H., and Gustafsson, B. (1983). Facilitated induction of hippocampal long-lasting potentiation during blockade of inhibition. *Nature* *307*, 603–604.

EXTENDED EXPERIMENTAL PROCEDURES

Mouse Genotyping

Mice were weaned at the third postnatal week and genotyped by PCR. Briefly, the mutant and corresponding WT alleles are detected by a four-primer PCR assay in which Oligo-1 (5'-GGAACCTTTGGAGCAATGGA-3') and Oligo-2 (5'-TGCCAATCAGAAAATCTAAAAC-3') give a WT band of 225 base-pair fragment and Oligo-3 (5'-TGTTCTGTGGCTATCAGGG-3') and Oligo-4 (5'-TGAGGAGTTCTTCTGAGGG-3') give a 432 base-pair fragment from the deleted allele.

Drugs

As indicated, the following drugs were added to ACSF superfusing slices: anisomycin (Calbiochem, CA), PKRi (Calbiochem, CA), diazepam (Sigma-Aldrich, St. Louis, MO), mouse IFN- γ (R & D systems, Minneapolis, MN), monoclonal Nab-IFN- γ (H22; R & D Systems, Minneapolis, MN) and bicuculline (Tocris, Ellisville, MO). The latter was bicuculline free base which blocks only GABA_A receptor (Debarbieux et al., 1998). D-amino-phosphonovalerate (D-AP5), 6-cyano-7-nitroquinoxaline-2,3-dione (CNQX), kynurenatate, picrotoxin and CGP55845 were all purchased from Tocris Bioscience (Ellisville, MO). PKRi (Calbiochem, San Diego), a potent ATP-binding-site-directed inhibitor of PKR activity (Jammi et al., 2003; Shimazawa and Hara, 2006) was applied to slices at a final concentration of 1 μ M (0.01% DMSO), which is known to block PKR activity *ex-vivo* (Page et al., 2006; Wang et al., 2007). For the *in vivo* studies PKRi was dissolved in saline and then injected intraperitoneally (i.p.) at a dose of 0.1 mg/kg, which is known to block PKR activity in the hippocampus *in vivo* (Ingrand et al., 2007). EEG was recorded 1 hr after PKRi injection.

LTP Experiments

Briefly, horizontal hippocampal slices (350 μ m) were cut from brains of WT or age-matched *Pkr*^{-/-} littermates in 4°C artificial cerebrospinal fluid (ACSF) and kept in ACSF at room temperature for at least one hr before recording. Slices were maintained in an interface-type chamber perfused with oxygenated ACSF (95% O₂ and 5% CO₂) containing in mM: 124 NaCl, 2.0 KCl, 1.3 MgSO₄, 2.5 CaCl₂, 1.2 KH₂PO₄, 25 NaHCO₃, and 10 glucose (2-3 ml/min). Bipolar stimulating electrodes were placed in the CA1 stratum radiatum to stimulate Schaffer collateral and commissural fibers. Field potentials were recorded at 28-29°C using ACSF-filled micropipettes. The recording electrodes were placed in the stratum radiatum for field excitatory postsynaptic potentials (fEPSPs), and stratum pyramidale for population spikes. The stimulus strength of the 0.1 ms pulses was adjusted to evoke 30%–35% of maximum response for fEPSPs, and 50% of maximal response for population spikes. A stable baseline of responses was established for at least 30 min at 0.033 Hz. Tetanic LTP was induced by high-frequency stimulation in brief trains (100 Hz for 1 s), applied either as a single train or four trains separated by 5 min intervals as previously described (Costa-Mattioli et al., 2007; Stoica et al., 2011). To reduce day-to-day variations, on a given day we recorded from WT and *Pkr*^{-/-} slices, or from slices of both groups treated with drugs. Furthermore, we recorded from WT and *Pkr*^{-/-} slices in parallel using only one slice per genotype (in the same chamber to ensure uniformity in experimental conditions across groups). Thus, the *n*'s refer to both the number of slices and the number of mice. Statistical analyses were performed with the *t* test and one-way ANOVA. All data are presented as means \pm SEM.

Elevated Plus Maze Test

The elevated plus-maze apparatus consisted of two open arms (35 \times 5 cm) and two enclosed arms of the same size (with 15 cm high opaque walls). The arms and central square were made of plastic plates and were elevated 40 cm above the floor. Mice were placed in the central square of the maze (5 \times 5 cm). Behavior was recorded during a 5 min period. Data acquisition and analysis were performed automatically with ANYMAZE software.

Open Field

Mice were placed in the center of a 40 \times 40 \times 40-cm arena, and their activity was quantified over a 10 min period by a computer-operated optical animal activity system (ANYMAZE).

Immunohistochemistry, Western Blotting, and ELISA

For immunohistochemical experiments mice were deeply anesthetized and perfused intracardially with cold PBS and subsequently with 4% paraformaldehyde (PFA) in ice cold 0.1 M phosphatase buffer (PBS). Brains were removed from the skull, stored in a 4% PFA solution overnight (at 4°C), and 40 μ m horizontal sections were cut on a microtome (Leica VT1000S, Germany). Free-floating method was used while rinsing between steps. Sections were first placed in a blocking solution (5% BSA, 0.3% Triton and 4% Normal Goat Serum in phosphate buffered saline) at room temperature for one hour, incubated overnight with primary antibodies [PKR (Santa Cruz Biotechnology, CA), GAD67 (Millipore, Billerica, MA), V-Glut 1 (Synaptic Systems, Goettingen, Germany) and PSD95 (NeuroMab, CA)] and then rinsed four times (for 20 min) with PBS before incubation with the secondary antibody (for 4 hr). After four washes (each for 20 min) with PBS, the sections were mounted on Superfrost Plus slides (VWR, West Chester, PA). Finally, the sections were coverslipped with VECTASHIELD® Hard Set mounting medium (Vector Lab, Burlingame, CA). Digital photos were taken with a Zeiss LSM 510 laser confocal microscope.

Egr-1 Staining

Prior to contextual fear conditioning, WT and *Pkr*^{-/-} mice were handled for three consecutive days. They were then trained as described above. Control groups were exposed to the context, except that they received no shock during training. Ninety minutes after training, brain sections were cut as described above and pre-treated in 0.3% H₂O₂ in PBS. The sections were incubated with an anti Egr-1 (1:7500) primary rabbit polyclonal antibody (Cell Signaling Technologies, Denver, MA) in a blocking solution (1% BSA, 0.3% triton and 4% normal goat serum in PBS) for 48 hr; and then incubated for 60 min at room temperature with a biotinylated goat-anti rabbit antibody (1:500; Vector Laboratories, Burlingame, CA) followed by an avidin–biotin–horseradish peroxidase (HRP; ABC kit; Vector Laboratories, Burlingame, CA). The bound peroxidase was located by incubating sections in 0.1% 3,3'-diaminobenzidine (DAB) and 0.025% H₂O₂ at room temperature for 5–10 min, which generated the visible substrate. Immunoreactive CA1 neurons were counted within a given area (0.07 mm²), as described earlier (Frankland et al., 2004; Hall et al., 2001).

ELISA

The hippocampi were dissected out of brain from WT and *Pkr*^{-/-} mice and homogenized in a buffer containing 320 mM sucrose, 5 mM HEPES, 1 mM NaHCO₃, 1 mM EDTA, 1 mM, 1% CHAPS, 0.5% BSA, 20 μg/ml PMSF, 20 μg/ml aprotinin. Homogenates were centrifuged at 12,000 rpm/min for 15 min at 4°C and the supernatant was recovered. The levels of murine IFN-γ production were determined by ELISA according to the manufacturer's procedure (R & D systems Minneapolis, MN).

SUPPLEMENTAL REFERENCES

- Costa-Mattioli, M., Gobert, D., Stern, E., Gamache, K., Colina, R., Cuello, C., Sossin, W., Kaufman, R., Pelletier, J., Rosenblum, K., et al. (2007). eIF2α phosphorylation bidirectionally regulates the switch from short- to long-term synaptic plasticity and memory. *Cell* 129, 195–206.
- Debarbieux, F., Brunton, J., and Charpak, S. (1998). Effect of bicuculline on thalamic activity: a direct blockade of IAHP in reticularis neurons. *J. Neurophysiol.* 79, 2911–2918.
- Frankland, P.W., Bontempi, B., Talton, L.E., Kaczmarek, L., and Silva, A.J. (2004). The involvement of the anterior cingulate cortex in remote contextual fear memory. *Science* 304, 881–883.
- Hall, J., Thomas, K.L., and Everitt, B.J. (2001). Fear memory retrieval induces CREB phosphorylation and Fos expression within the amygdala. *Eur. J. Neurosci.* 13, 1453–1458.
- Ingrand, S., Barrier, L., Lafay-Chebassier, C., Fauconneau, B., Page, G., and Hugon, J. (2007). The oxindole/imidazole derivative C16 reduces in vivo brain PKR activation. *FEBS Lett.* 581, 4473–4478.
- Jammi, N.V., Whitby, L.R., and Beal, P.A. (2003). Small molecule inhibitors of the RNA-dependent protein kinase. *Biochem. Biophys. Res. Commun.* 308, 50–57.
- Page, G., Rioux Bilan, A., Ingrand, S., Lafay-Chebassier, C., Pain, S., Perault Pochat, M.C., Bouras, C., Bayer, T., and Hugon, J. (2006). Activated double-stranded RNA-dependent protein kinase and neuronal death in models of Alzheimer's disease. *Neuroscience* 139, 1343–1354.
- Shimazawa, M., and Hara, H. (2006). Inhibitor of double stranded RNA-dependent protein kinase protects against cell damage induced by ER stress. *Neurosci. Lett.* 409, 192–195.
- Stoica, L., Zhu, P.J., Huang, W., Zhou, H., Kozma, S.C., and Costa-Mattioli, M. (2011). Selective pharmacogenetic inhibition of mammalian target of Rapamycin complex I (mTORC1) blocks long-term synaptic plasticity and memory storage. *Proc. Natl. Acad. Sci. USA* 108, 3791–3796.
- Wang, X., Fan, Z., Wang, B., Luo, J., and Ke, Z.J. (2007). Activation of double-stranded RNA-activated protein kinase by mild impairment of oxidative metabolism in neurons. *J. Neurochem.* 103, 2380–2390.

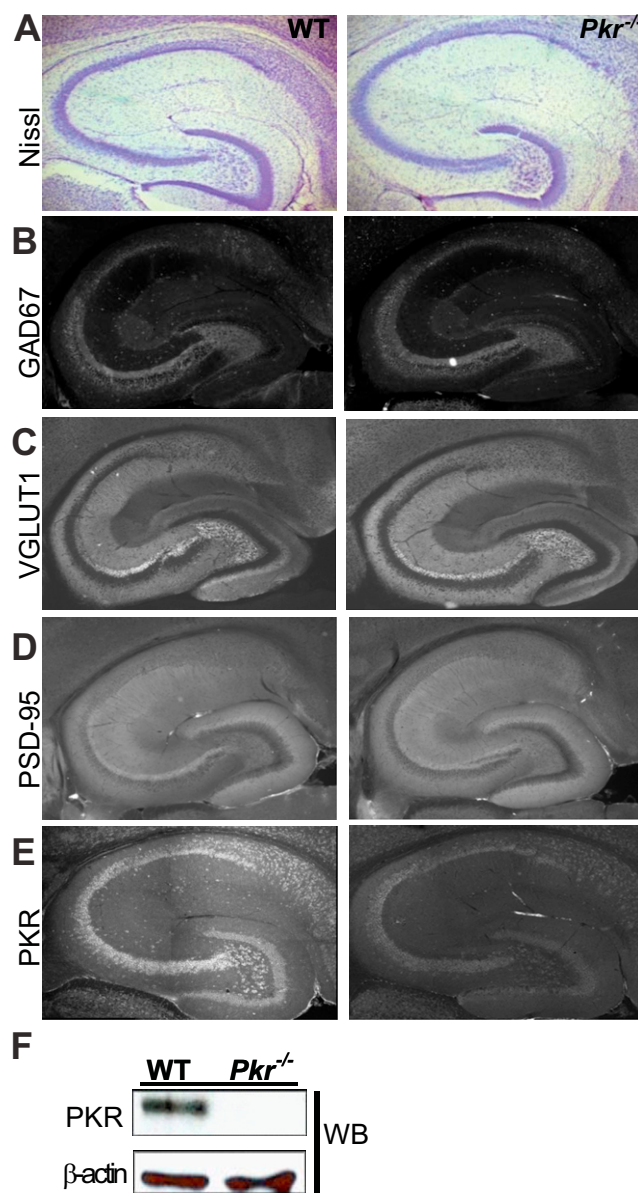


Figure S1. Lack of *Pkr* Does Not Alter Gross Brain Morphology, Related to Figures 1 and 2

(A–E) Horizontal hippocampal sections from WT and *Pkr*^{-/-} mice were stained with Nissl stain (A) or with antibodies against GAD67 (B), VGLUT1 (C), PSD95, or (D) PKR (E).

(F) Note no major difference between WT and *Pkr*^{-/-} mice, except for absence of PKR staining, which was confirmed by Western blotting.

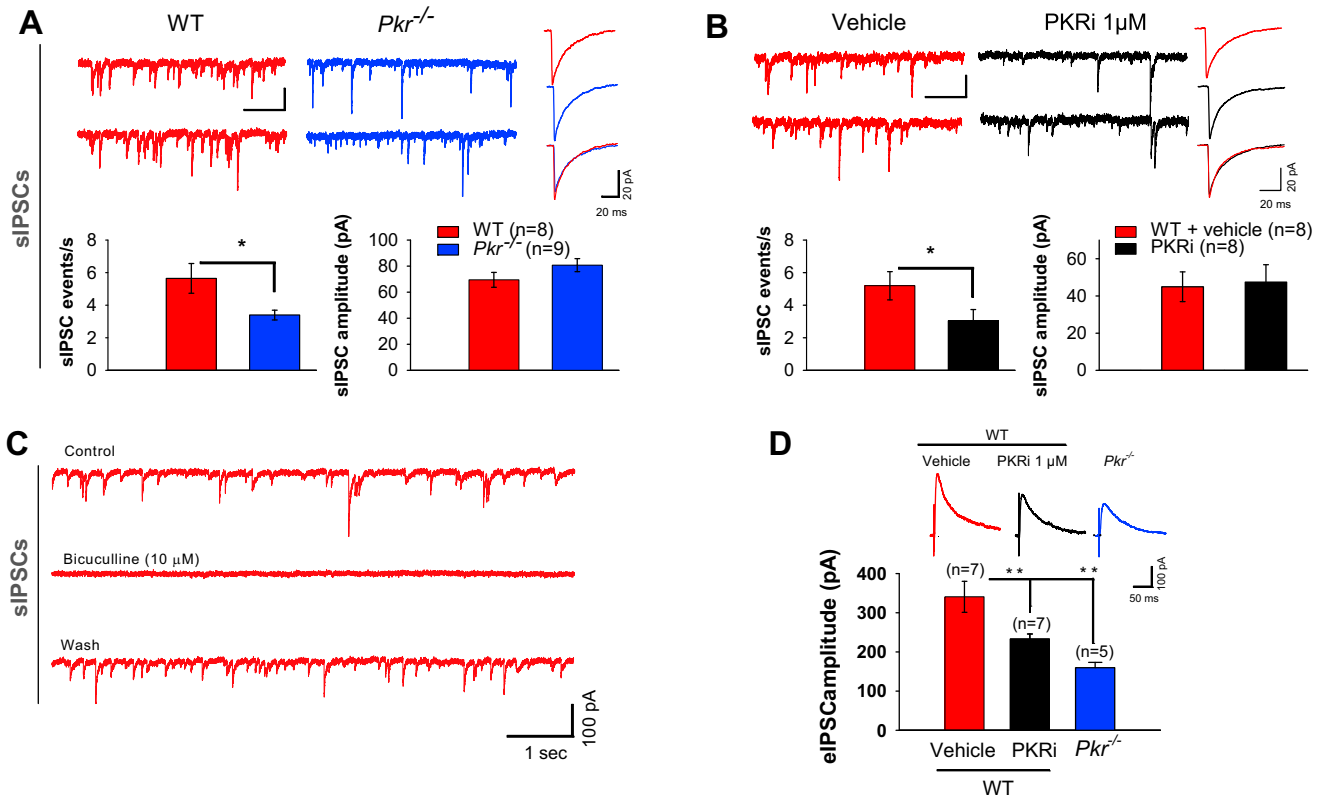


Figure S2. sIPSCs and eIPSCs Are Reduced in CA1 from *Pkr*^{-/-} Mice and WT Slices Treated with PKRi, Related to Figure 3

(A) Sample traces (top) and summary data (bottom) show reduced frequency (Mann-Whitney U test, $U = 14.4$; $*p < 0.05$) but no change in amplitude of sIPSCs ($t = 1.18$; $p = 0.22$) in *Pkr*^{-/-} slices (recorded at -60 mV in the presence of 2 mM kynurenic acid). Traces at right (each is an average of at least 100 events) do not differ between WT slices (uppermost) and *Pkr*^{-/-} slices (middle), as confirmed by superimposed traces (lowest).

(B) Similarly, in WT slices, PKRi decreases sIPSCs frequency (Mann-Whitney U test, $U = 12.7$; $*p < 0.05$) but not amplitude ($t = 0.16$; $p = 0.88$). Summary data and individual events are as in (A).

(C) Reversible elimination of sIPSCs in WT slices by bicuculline confirms their mediation by GABA_A receptors.

(D) Electrically isolated half-maximal evoked IPSCs (eIPSCs), recorded at 0 mV with gluconate-containing pipettes, were consistently smaller in *Pkr*^{-/-} slices (Mann-Whitney U test, $U = 0.0$; $*p < 0.01$) and WT slices treated with PKRi (Mann-Whitney U test, $U = 0.0$; $*p < 0.01$).

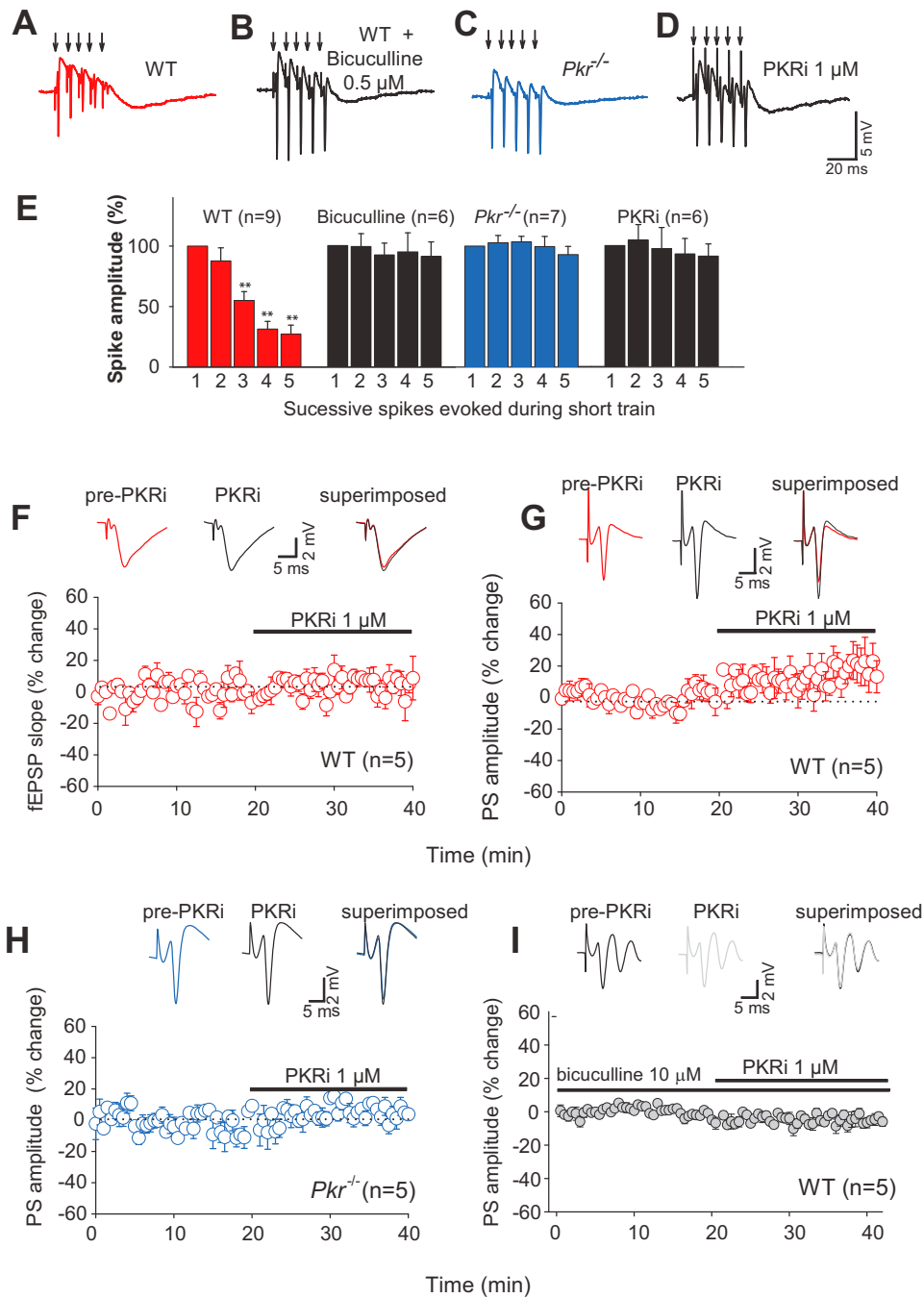


Figure S3. Cumulative Inhibition Is Reduced in *Pkr*^{-/-} Slices or WT Slices Treated with PKRi, Related to Figures 2 and 3

(A–E) During brief high frequency stimulation (5 pulses at 100 Hz), population spikes decay rapidly in WT slices, owing to cumulative GABAergic inhibition (A; $p < 0.01$); but not in *Pkr*^{-/-} slices (B; $p > 0.05$) or WT slices treated with either bicuculline (C; $p > 0.05$) or PKRi (D; $p > 0.05$). Data are summarized in E.

(F–H) PKRi specifically enhances single population spikes elicited by reducing GABAergic inhibition. PKRi did not alter presynaptic afferent volley or the initial slope of EPSPs (F; $t = 1.02$, $p = 0.34$); but increased the amplitude of population spikes in WT slices (G, $t = 2.98$; $p < 0.05$) but not in *Pkr*^{-/-} slices (H; $t = 1.77$; $p = 0.12$). (I) In bicuculline-treated WT slices PKRi caused no further enhancement of firing, as expected if PKRi acts by reducing GABAergic inhibition ($t = 0.69$; $p = 0.51$).

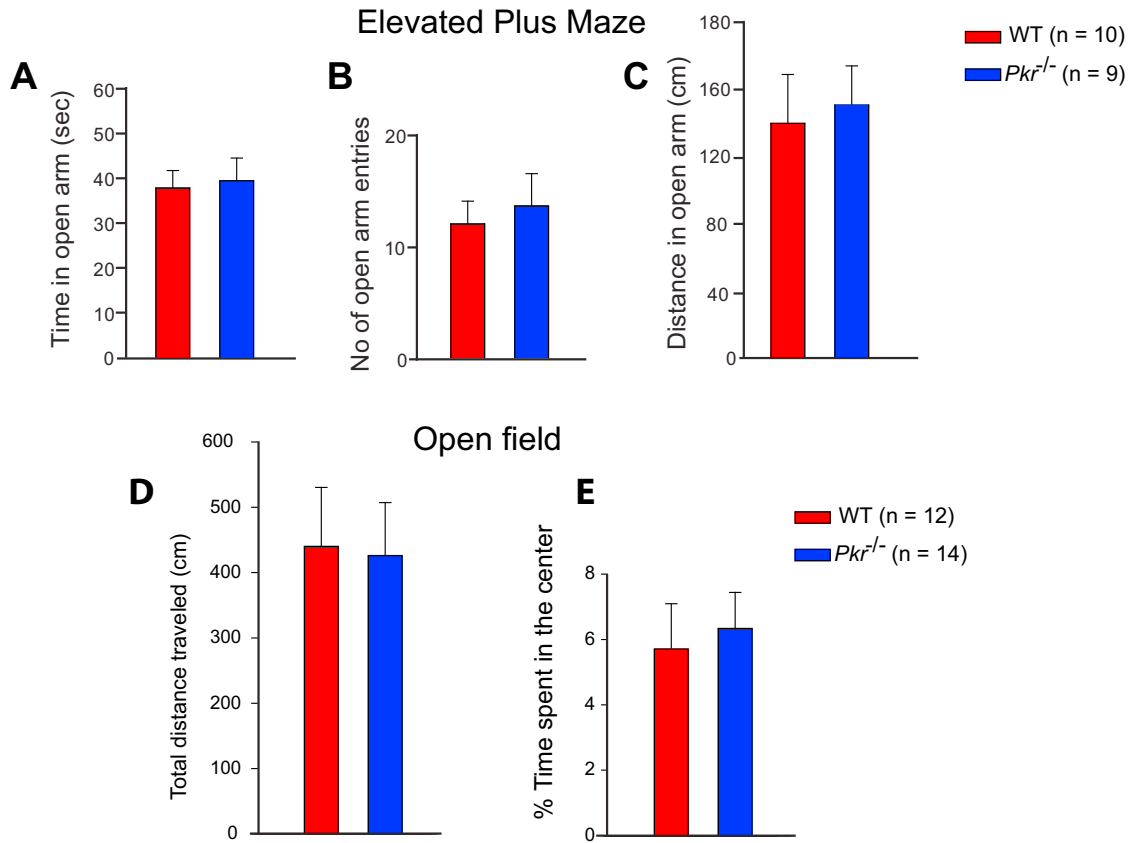


Figure S4. *Pkr*^{-/-} Mice Behave Normally in the Elevated Plus Maze and Open Field, Related to Figure 6

(A–E) Time spent in the less secure open arm (A; $F_{(1,17)} = 0.73$; $p = 0.8$), number of open arm entries (B; $F_{(1,17)} = 0.21$; $p = 0.7$), and distance traveled in the open arm (C; one-way ANOVA Ranks, $p = 0.3$) did not significantly differ between WT and *Pkr*^{-/-} mice. WT and *Pkr*^{-/-} mice traveled a similar total distance (D; $F_{(1,24)} = 0.05$; $p = 0.9$) and spent similar time in the center of the open field (E; one-way ANOVA Ranks, $p = 0.6$).

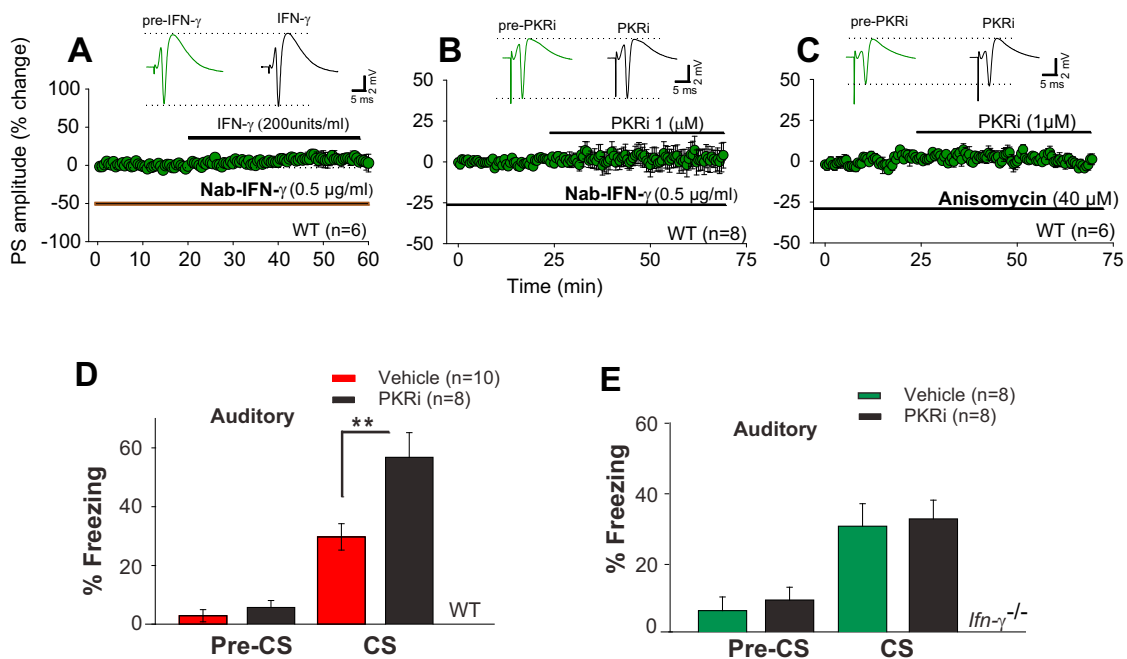


Figure S5. PKRi Enhances Population Spikes and Long-Term Auditory Fear Memory in WT Mice, but Not *Ifn- γ* -Deficient Mice, Related to Figure 7

(A and B) In presence of NAb-IFN- γ , exogenous IFN- γ (A), $t = 0.32$; $p = 0.262$) or PKRi (B), $t = 0.18$; $p = 0.860$) did not significantly alter population spike amplitude. (C) Anisomycin blocked the PKRi-induced increase in population spike amplitude ($t = 0.0519$; $p = 0.960$).

(D and E) Injection of PKRi (0.1 mg/kg i.p.) immediately after training enhanced long-term auditory fear memories in WT mice (D, $F_{(1,16)} = 9.1$; $**p < 0.01$) but had no effect in *Ifn- γ* ^{-/-} mice (E, $F_{(1,14)} = 0.06$; $p = 0.81$). Freezing times were measured 24 hr post-training, either before the onset of the tone (pre-CS, for 2 min) or during the tone presentation (for 3 min).

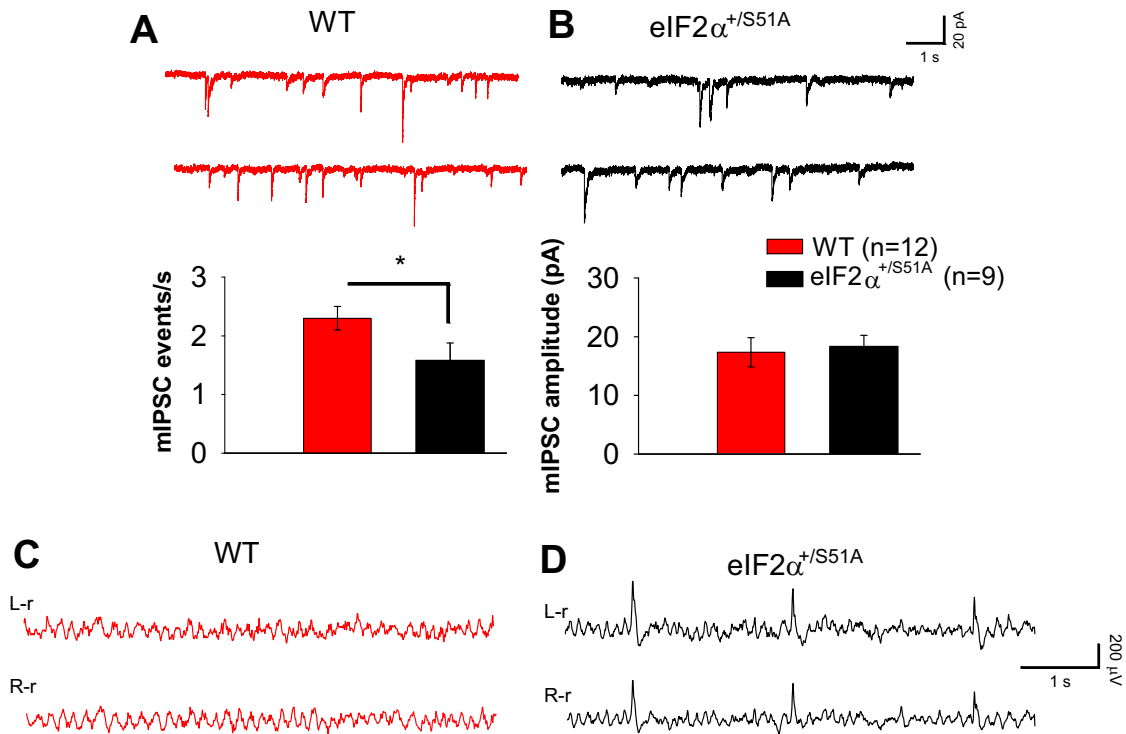


Figure S6. Reduced Inhibition and Increased Synchronized EEG Activity in eIF2 $\alpha^{+/S51A}$ Mice, Related to Figure 3 and Figure 1

(A and B) Sample traces (top) and summary data (bottom) show reduced frequency ($t = 2.35$; $*p < 0.05$) but no change in the amplitude ($t = 1.15$; $p = 0.285$) of mIPSCs in eIF2 $\alpha^{+/S51A}$ slices (A), compared to WT slices (B) [recorded at -60 mV with KCl containing patch pipette in the presence of kynurenatate (2 mM) and tetrodotoxin (TTX, 1 μ M)].

(C and D) Traces from bilateral cortical electrodes (left hemisphere-reference, L-r; right hemisphere-reference, R-r) show interictal spiking in eIF2 $\alpha^{+/S51A}$ mice (D) but not in WT controls (C). Abnormal EEG activity was absent from all WT littermates recordings ($n = 4$), but present in all eIF2 $\alpha^{+/S51A}$ mice ($n = 5$); by Fisher's exact test, $p < 0.01$.

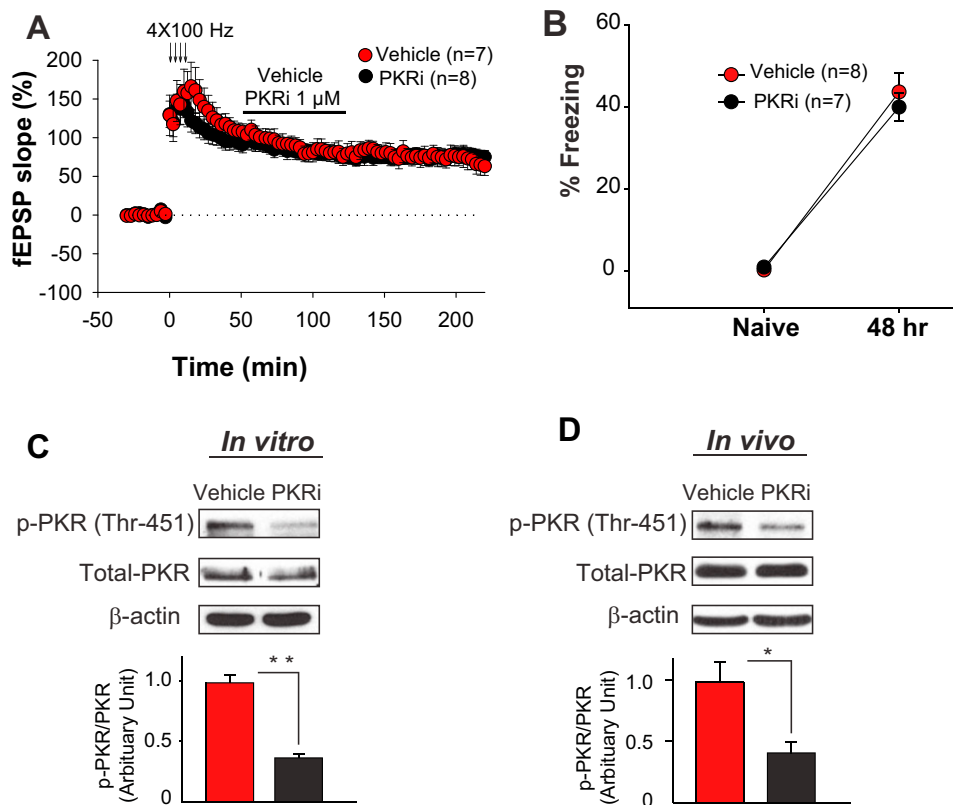


Figure S7. PKRi Has No Effect on L-LTP and LTM Maintenance, but It Reduces PKR Activity in CA1, Both in Slices and In Vivo, Related to Figures 5 and 6

(A) In WT slices, PKRi applied 60 min after tetanic stimulation did not alter L-LTP maintenance ($F_{(1,13)} = 0.13$; $p = 0.74$).

(B) PKRi i.p.-injected one day after fear conditioning did not affect memory retention tested the next day (at 48 hr; $F_{(1, 15)} = 0.29$; $p = 0.61$).

(C) WT slices were vehicle- or PKRi-treated for 20 min and PKR activity was determined by Western blotting, using a phospho-specific antibody (Thr-451).

(D) Vehicle or PKRi was injected i.p., the hippocampus was isolated 30 min later and PKR activity was determined as in (A). Plots (below) show quantification of normalized p-PKR using total-PKR as loading control (for each group, $n = 3$; A, $t = 7.56$; $**p < 0.01$; (B), $t = 2.96$, $*p < 0.05$).